

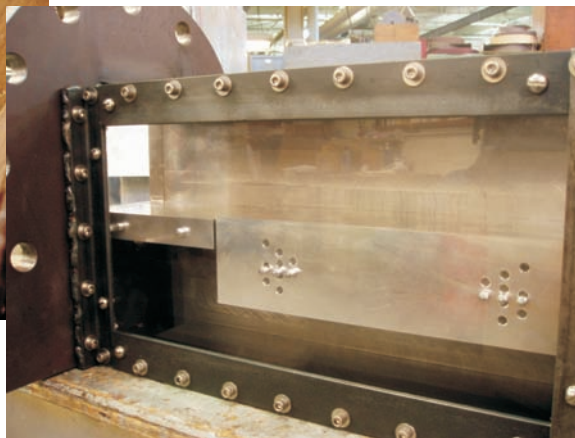
RECLAMATION

Managing Water in the West

Report DSO-07-07

Uplift and Crack Flow Resulting from High Velocity Discharges Over Open Offset Joints

Laboratory Studies



Dam Safety Technology Development Program



U.S. Department of the Interior
Bureau of Reclamation
Technical Service Center
Denver, Colorado

December 2007

REPORT DOCUMENTATION PAGE

*Form Approved
OMB No. 0704-0188*

The public reporting burden for this collection of information is estimated to average 1 hour per response, including the time for reviewing instructions, searching existing data sources, gathering and maintaining the data needed, and completing and reviewing the collection of information. Send comments regarding this burden estimate or any other aspect of this collection of information, including suggestions for reducing the burden, to Department of Defense, Washington Headquarters Services, Directorate for Information Operations and Reports (0704-0188), 1215 Jefferson Davis Highway, Suite 1204, Arlington, VA 22202-4302. Respondents should be aware that notwithstanding any other provision of law, no person shall be subject to any penalty for failing to comply with a collection of information if it does not display a currently valid OMB control number.

PLEASE DO NOT RETURN YOUR FORM TO THE ABOVE ADDRESS.

1. REPORT DATE (DD-MM-YYYY) 12-2007		2. REPORT TYPE		3. DATES COVERED (From - To)	
4. TITLE AND SUBTITLE Uplift and Crack Flow Resulting from High Velocity Discharges over Open Offset Joints—Laboratory Studies				5a. CONTRACT NUMBER	
				5b. GRANT NUMBER	
				5c. PROGRAM ELEMENT NUMBER	
6. AUTHOR(S) Frizell, Warren				5d. PROJECT NUMBER	
				5e. TASK NUMBER	
				5f. WORK UNIT NUMBER	
7. PERFORMING ORGANIZATION NAME(S) AND ADDRESS(ES) Bureau of Reclamation Technical Service Center Water Resources Research Laboratory Group Denver, Colorado				8. PERFORMING ORGANIZATION REPORT NUMBER DSO-07-07	
9. SPONSORING/MONITORING AGENCY NAME(S) AND ADDRESS(ES) Bureau of Reclamation Denver, Colorado				10. SPONSOR/MONITOR'S ACRONYM(S)	
				11. SPONSOR/MONITOR'S REPORT NUMBER(S) DSO-07-07	
12. DISTRIBUTION/AVAILABILITY STATEMENT National Technical Information Service, 5285 Port Royal Road, Springfield, VA 22161					
13. SUPPLEMENTARY NOTES					
14. ABSTRACT					
15. SUBJECT TERMS					
16. SECURITY CLASSIFICATION OF:			17. LIMITATION OF ABSTRACT SAR	18. NUMBER OF PAGES	19a. NAME OF RESPONSIBLE PERSON
a. REPORT UL	b. ABSTRACT UL	a. THIS PAGE UL			19b. TELEPHONE NUMBER (Include area code)

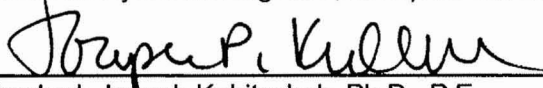
BUREAU OF RECLAMATION
Technical Service Center, Denver, Colorado
Water Resources Research Laboratory Group, 86-68560

Report DSO-07-07

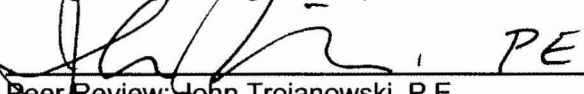
**Uplift and Crack Flow Resulting from
Discharges over Open Offset Joints
Laboratory Studies**

**Dam Safety Technology Development Program
Denver, Colorado**


Prepared: K. Warren Frizell
Research Hydraulic Engineer, Group 86-68560


Checked: Joseph Kubitschek, Ph.D., P.E.
Hydraulic Engineer, Group 86-68560


Technical Approval: Robert Einhellig, P.E.
Acting Group Manager, Group 86-68560

 PE
Peer Review: John Trojanowski, P.E.
Civil Engineer, Group 86-68130

1/30/08
Date

REVISIONS					
Date	Description	Prepared	Checked	Technical Approval	Peer Review

Mission Statements

The mission of the Department of the Interior is to protect and provide access to our Nation's natural and cultural heritage and honor our trust responsibilities to Indian Tribes and our commitments to island communities.

The mission of the Bureau of Reclamation is to manage, develop, and protect water and related resources in an environmentally and economically sound manner in the interest of the American public.

Acknowledgments

Reclamation's Dam Safety Technology Development Program supported this work. Thanks to Nate Snortland for providing continued support through this entire process. Joe Kubitscheck, with some assistance from Billy Baca, both of the Water Resources Research Laboratory, carried out the laboratory particle image velocimetry (PIV) measurements. Joe Kubitscheck also was the checker and provided many excellent comments on this report. Jim Higgs, also of the Water Resources Research Laboratory performed the computational fluid dynamics (CFD) computer runs using Flow-3D. John Trojanowski of the Concrete Dams and Waterways Group served as the peer reviewer and has added many beneficial comments regarding direction of the studies throughout the project.

Contents

	Page
Acknowledgments.....	iii
Executive Summary	1
Introduction.....	2
Experimental Methods.....	5
Laboratory Model	5
Numerical Model	9
Model Description	10
Prototype Spillway Chute Simulation.....	11
Laboratory Model Simulation.....	12
Results.....	12
Laboratory Model	12
Sharp-Edged Crack.....	12
Chamfer-Edged Crack	18
Radius-Edged Crack	24
General Trends.....	29
Particle Image Velocity.....	30
Numerical Modeling.....	37
Prototype Chute CFD Modeling.....	37
Laboratory Test Facility CFD Modeling	44
Discussion.....	50
Conclusions and Recommendations	53
References.....	54

Tables

No.	Page
1 Coefficients of power curve fits for sharp-edged geometry. Equation is in the form $P = a U^b$, where U is the velocity and P is the uplift pressure (sealed or vented).....	14
2 Coefficients of power curve fits for chamfer-edged geometry. Equation is in the form $P = a U^b$, where U is the velocity and P is the uplift pressure (sealed or vented).....	20
3 Coefficients of power curve fits for radius-edged geometry. Equation is in the form $P = a U^b$, where U is the velocity and P is the uplift pressure (sealed or vented).....	26

Figures

No.	Page
1	3
2	4
3	4
4	5
5	6
6	7
7	7
8	8
9	10
10	11
11	13
12	14
13	15
14	15
15	16
16	16
17	17
18	17
19	18
20	19
21	19
22	20
23	21
24	21
25	22
26	22

27 Mean uplift pressure, chamfer-edged geometry, vented cavity, 1/2-inch gap..... 23

28 Unit discharge through joint/crack, chamfer-edged, 1/2-inch gap..... 23

29 Mean uplift pressure, radius-edged geometry, sealed cavity, 1/8-inch gap.... 24

30 Mean uplift pressure, radius-edged geometry, vented cavity, 1/8-inch gap. .. 25

31 Unit discharge through joint/crack, radius-edged, 1/8-inch gap..... 25

32 Mean uplift pressure, radius-edged, sealed cavity, 1/4-inch gap..... 26

33 Mean uplift pressure, radius-edged geometry, vented cavity, 1/4-inch gap. .. 27

34 Unit discharge through joint/crack, radius-edged, 1/4-inch gap..... 27

35 Mean uplift pressure, radius-edged geometry, sealed cavity, 1/2-inch gap.... 28

36 Mean uplift pressure, radius-edged geometry, vented cavity, 1/2-inch gap. .. 28

37 Unit discharge through joint/crack, radius-edged geometry, 1/2-inch gap..... 29

38 Velocity fields for the 1/8-inch gap and 1/2-inch chamfered offset at 20-ft/s free stream velocity test conditions: (a) vented and (b) sealed cavity. 31

39 Velocity fields for the 1/8-inch gap and 1/2-inch chamfered offset at 30-ft/s free stream velocity test conditions: (a) vented and (b) sealed cavity. 32

40 Velocity fields for the 1/2-inch gap and 1/2-inch chamfered offset at 20-ft/s free stream velocity test conditions: (a) vented and (b) sealed cavity. 33

41 Velocity fields for the 1/2-inch gap and 1/2-inch chamfered offset at 30-ft/s free stream velocity test conditions: (a) vented and (b) sealed cavity. 34

42 Joint/crack velocity profiles for the vented 1/8-inch gap configuration with test velocities of 20 and 30 ft/s. 36

43 Joint/crack velocity profiles for the vented 1/2-inch gap configuration with test velocities of 20 and 30 ft/s. 36

44 Prototype chute CFD model results, 12-inch flow depth, 10 ft/s velocity, 1/8-inch offset into the flow, 1/8-inch joint/crack gap, sealed cavity. Pressures are in lb/ft², and velocity in ft/s..... 38

45 Prototype chute CFD model results, 12-inch flow depth, 50 ft/s velocity, 1/8-inch offset into the flow, 1/8-in joint/crack gap, sealed cavity. Pressures are in lb/ft², and velocity in ft/s..... 39

46 Prototype chute CFD model results, 12-inch flow depth, 90 ft/s velocity, 1/8-inch offset into the flow, 1/8-inch joint/crack gap, sealed cavity. Pressures are in lb/ft², and velocity in ft/s. Pressures are in lb/ft², and velocity in ft/s. 40

47 Prototype chute CFD model results, 12-inch flow depth, 10 ft/s velocity, 1/8-inch offs Pressures are in lb/ft², and velocity in ft/s.et into the flow, 1/8-inch joint/crack gap, flow in joint/crack to atmospheric pressure (worst case). 41

48 Prototype chute CFD model results, 12-inch flow depth, 50 ft/s velocity, 1/8-inch offset into the flow, 1/8-inch joint/crack gap, flow in joint/crack to atmospheric pressure (worst case). Pressures are in lb/ft², and velocity in ft/s. 42

49 Prototype chute CFD model results, 12-inch flow depth, 90 ft/s velocity, 1/8-inch offset into the flow, 1/8-inch joint/crack gap, flow in joint/crack to atmospheric pressure (worst case). Pressures are in lb/ft², and velocity in ft/s. 43

50	Unit discharge in joint/crack for 1/8-inch offset and 1/8-inch gap. Free surface simulation with 1-foot depth.	44
51	Laboratory test facility CFD results for a 1/32-inch gap with 1/8-inch offset into the flow for a 50 ft/s velocity. Pressure is in lb/ft ² and velocity in ft/s.	45
52	Flow3D simulation of 1/16-inch gap with 1/8-inch offset into the flow for a 50-ft/s velocity. Pressure is in lb/ft ² and velocity in ft/s.....	46
53	Flow3D simulation of 1/8-inch gap with 1/8-inch offset into the flow for a 50-ft/s velocity. Pressure is in lb/ft ² and velocity in ft/s.....	47
54	Flow3D simulation of 1/4-inch gap with 1/8-inch offset into the flow for a 50-ft/s velocity. Pressure is in lb/ft ² and velocity in ft/s.....	48
55	Flow3D simulation of 1/2-inch gap with 1/8-inch offset into the flow for a 50-ft/s velocity. Pressure is in lb/ft ² and velocity in ft/s.....	49
56	Graph derived from Johnson's work in 1976 on uplift of steep chute lateral linings.....	51

Executive Summary

This report describes laboratory tests that were completed to extend the available data on uplift pressures generated by high velocity flows over offset joints. In addition, magnitudes of flows into the joints or cracks were measured for various configurations. Lab data were supplemented with numerical modeling using the computer program, Flow-3D.

Three joint geometries were tested: sharp (90-degree) edges, $\frac{1}{8}$ -inch chamfered (45-degree) edges, and edges with a $\frac{1}{8}$ -inch radius in combinations of joint/crack gaps ranging from $\frac{1}{8}$ -inch to $\frac{1}{2}$ -inch and offsets into the flow ranging from $\frac{1}{8}$ -inch to $\frac{3}{4}$ -inch. Velocities ranging from about 10 ft/s up to 55 ft/s were tested. The effects of orientation of the joint to the flow was also tested; however due to geometry restrictions of the test channel, joints perpendicular to the flow received the majority of attention for this effort.

Mean pressure differentials across the plate downstream from the offset were measured for all cases. The cavity beneath the test section could be closed, generating the maximum uplift, or opened to allow flow to enter the cavity through the joint/crack. This test facility feature allowed for measurement of a slightly reduced uplift pressure and flow rates through the open joint/crack area. These flow rate data are representative of a fixed head loss, as the exit piping remained constant throughout the testing.

Uplift pressure and flow rate data from this study will be used to reduce the uncertainty in analyses used during risk assessments to provide improved estimates of the level of effort required to bring a spillway or outlet works into a safe operating condition for a variety of geometries.

Introduction

Flow-driven uplift forces in hydraulic structures historically have been a common topic of interest for safe and reliable design. The majority of research has focused on lined and unlined plunge pools subject to free-falling water jets from spillways or outlets. The transmission of dynamic pressures from plunging jet decay depends on many jet-related characteristics; the jet geometry, breakup length, and length of fall through the atmosphere, the depth of the water in the plunge pool, and the amount of air entrainment are a few of the more important parameters. In addition, the transmission of pressures beneath engineered plunge pool slabs or into a fissured rock matrix depends largely on joint location, geometry, and design (water stops). Bollaert (2002) has documented the generation of significant uplift pressures in both lined and unlined basins with open joints by detailing the generation of large dynamic pressures, especially when air entrainment is present, and their effect on scour in unlined rock basins subject to jet impingement. In a related study, Melo et al. (2006) discuss the influence of joint location and geometry in concrete-lined plunge pools subjected to jet impact. Numerous other researchers have also contributed to the overall understanding of the physical processes affecting uplift and rock scour.

The purpose of this document is to describe recent investigations that address unknowns related to uplift pressures and resulting flows into cracks and joints caused by high velocity chute-supported flows. Such flow conditions have been less studied; however, it is a common problem that can occur in spillways and outlet works of various sizes, types, and head ranges. The uplift force in a chute-supported flow can consist of a component due to reduced pressures on the flow surface of a slab caused by flow separation resulting in a localized pressure reduction, and the transfer of dynamic pressures to the lower side of the slab through an open crack or joint. In addition, there is also the possibility of uplift forces due to excess leakage or piping from the reservoir in the foundation material of the chute. Uplift on chute slabs due to the transmission of pressure through open cracks and/or joints has long been an area of concern at the Bureau of Reclamation (Reclamation), and damage has occurred on numerous occasions due to this phenomenon. Hepler and Johnson (1988) described typical analysis of spillway failures due to uplift and discussed case studies within Reclamation. Johnson (1976) performed a model study depicting a two-dimensional open channel flow on a steep canal wasteway with a range of offsets and gap dimensions. Johnson did not model flow through the joint but did measure uplift pressures resulting from a variety of offset dimensions (both vertical and horizontal) for flows up to about 15 ft/s. Trojanowski (2004) identified erosion of foundation materials resulting from flows into cracks or joints as a significant problem for spillways on soil foundations. Prior to this study, there were no simple methods for predicting these flows. The results of this study extend uplift

pressure data to include velocities in the range of 10 to 55 ft/s and provide additional information concerning crack flow rate.

In typical reinforced concrete-lined chutes, the stability of the slabs depends on the overall concrete design; including joint and waterstop details, reinforcement, anchorage, and a functioning, filtered underdrain system. Usually, drainage under the slab is provided to prevent the buildup of uplift pressure and subsequent instability due to seepage and natural foundation groundwater conditions. Typically, damage resulting from hydrodynamic uplift on slabs begins at the joints, where offsets or spalling has occurred (fig. 1). Spillway flows over these offsets can introduce water into the foundation, which can lead to structural damage due to uplift or erosion of the foundation material. If this problem persists, there can be complete failure and removal of chute slabs (fig. 2). Reclamation has used predictive data to evaluate potential uplift problems; however, sufficient methods, specific to estimating the amount of flow into cracks or joints that could be possible, have not been developed primarily due to limited availability of data. This problem is generally more of a concern for structures where the chute and the underdrain systems may be in poor condition due to aging or improper design and is especially critical for chutes that are founded on soil, since joint/crack flow can lead to erosion and undermining (fig. 3) of the chute foundation and structural collapse of a chute slab (fig. 4).



Figure 1.—Initial damage due to uplift generally occurs at the construction joints.

Uplift and Crack Flow Resulting from
High Velocity Discharges over Open Offset Joints



Figure 2.—If flow is allowed to continue, slabs may lift resulting in wild spray and rooster tails, and when the water recedes - slabs are damaged or missing.



Figure 3.—Undermining of the chute slab has occurred due to flow entering at joints and cracks and transporting foundation material through unfiltered drains.



Figure 4.—Structural collapse of the slab system occurs when enough undermining has occurred to cause loss of support. This damage is typical of slabs placed on soil foundations (note: this slab is not reinforced so failure is more evident).

With the advent of the risk assessment process as an approach to assist dam safety decision makers in determining if repairs or replacement of hydraulic structures is needed, Reclamation engineers have identified a critical need for additional data that would allow reduced uncertainty in the prediction of possible uplift or structural collapse failure modes. The data presented in this report should extend the available data on uplift and provide new estimates of crack and joint flows that have previously been unavailable. It is the intent of the author that simple spreadsheet tools can then be developed to assist in making these predictions in a timely manner, with more certainty, and ultimately lead to wiser use of the limited financial resources that project owners are faced with.

Experimental Methods

Laboratory Model

Representing high velocity flows, typical of a spillway chute, over offset joints or cracks in a laboratory setting can pose difficulties. In addition to providing relatively deep, high-velocity, open channel flow that requires large flow rates, the dimensions of joint/crack gaps and offsets can be relatively small in

Uplift and Crack Flow Resulting from High Velocity Discharges over Open Offset Joints

comparison with overall spatial scales for the prototype structure. While gravitational and inertial forces typically dominate open channel flows, viscous and inertial forces dominate physical processes involving flow through small cracks or joints along a channel boundary. These issues point toward using a full scale representation of the joint/crack details to ensure the measured joint/crack flows and pressures are free from scale effects related to viscous forces (i.e., requires Reynolds number similitude).

The test setup for this study comprised a sectional representation with prototype joint/crack gaps, offsets, and velocities (10 to 55 ft/s) using a water tunnel connected to the laboratory's high-head pump facility. This facility has the ability to generate a moderate flow rate ($6 \text{ ft}^3/\text{s}$) at heads approaching 600 feet and, with proper design of the water tunnel test section, is capable of producing velocities up to about 55 ft/s. Figure 5 shows a plan view schematic diagram of the overall layout. The test section (fig. 6) features a 4-inch wide by 4-inch high square cross-sectional geometry. While not a true representation of open channel flow, the forces dominating the processes in this problem, as previously mentioned, are not gravity driven; hence flow depths are not a critical component, and the closed conduit flow approximation can be applied.

Flow entering the test section was measured with a venturi meter and mercury manometer to reproduce testing set-points and determine mean test section velocities ($U = Q/A$, where U is the mean velocity through the test section, Q is the volumetric flow rate, and A is the test section cross-sectional area). Mean differential pressures across the slab downstream from the joint/crack offset were measured with a Sensotec Model A-5 differential pressure transducer rated at 15 pounds per square inch differential (psid). The output was a Model GM that supplied excitation to the sensor and featured a 0- to 5-V output (full scale). The amplifier/display used a shunt calibration feature that was periodically checked and adjusted throughout testing. Figure 7 shows the location of the pressure measurement and details the flow splits. The voltage output was read using a Wavebook 516 and a laptop PC. Data were anti-alias filtered and collected at

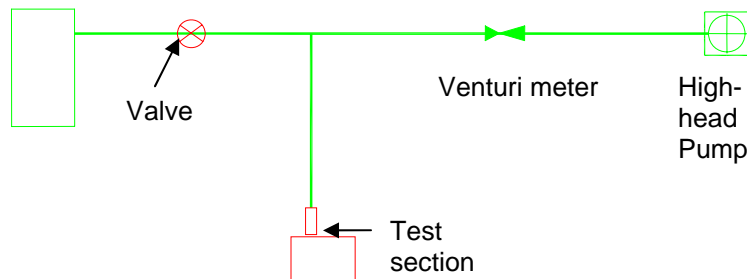


Figure 5.—Plan view schematic of model layout showing pump, piping, valve, and test section.

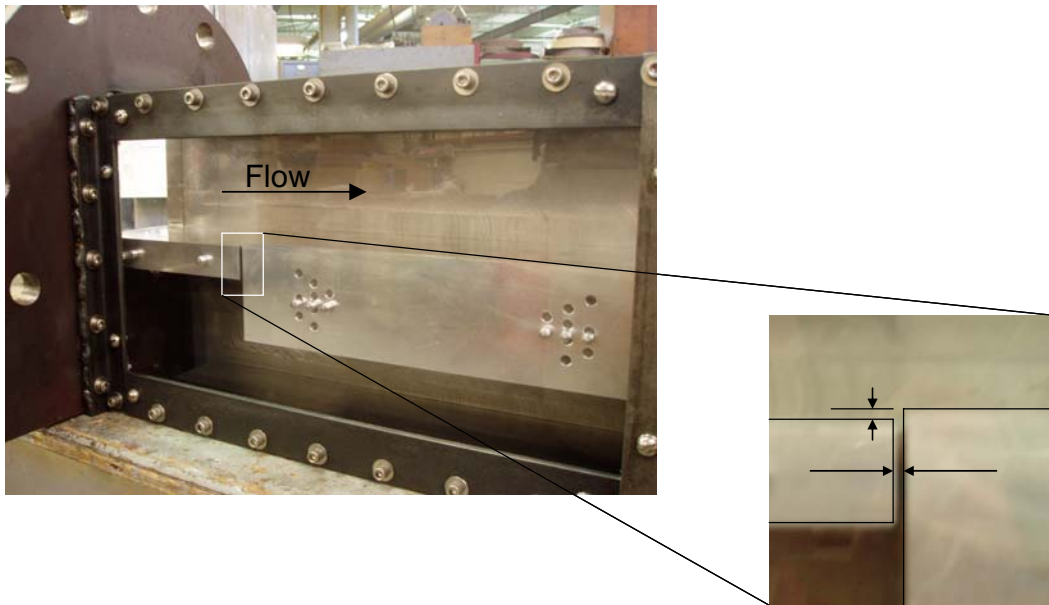


Figure 6.—Laboratory model test section. Note detail of offset and joint/crack gap.

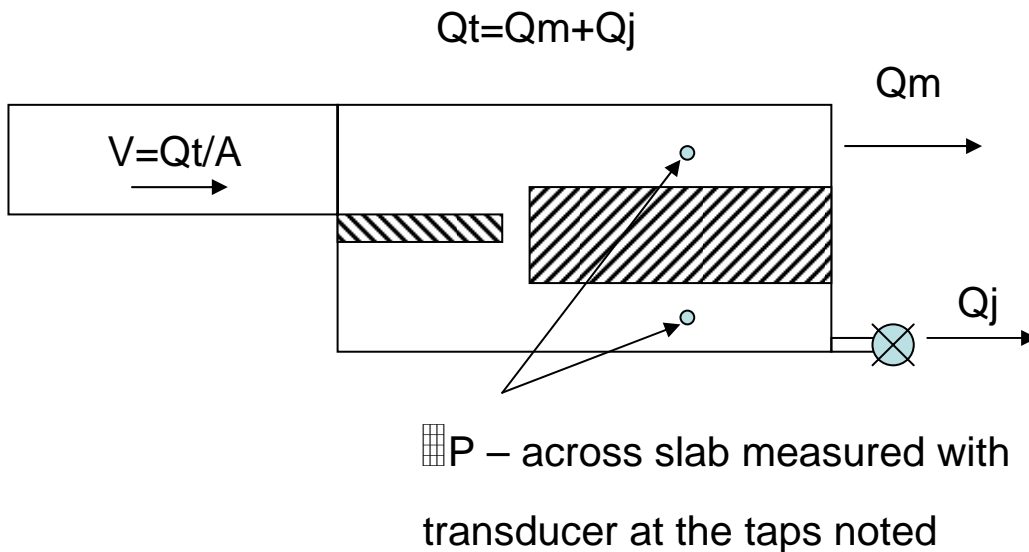


Figure 7.—Side-view schematic of test section showing location of uplift pressure taps.

200 Hz for 50 seconds and then time-averaged. This was done both with the lower cavity sealed, and with it open to allow flow through the joint/crack. Volumetric flow rates through the joint/crack were initially measured using the mean of 5 tests from a volume/time method. This check was performed at a couple of joint/crack gaps. The flow rate was then correlated with the difference in the differential pressure between the sealed- and open-cavity conditions for given test configurations, using physically based theory. The resulting correlation allowed use of only the measurement of the differential pressures in order to

Uplift and Crack Flow Resulting from High Velocity Discharges over Open Offset Joints

deduce the joint/crack discharge. Each joint/crack configuration was tested for a range of test section velocities from about 15 ft/s to 55 ft/s. The velocity was computed using the measured discharge and cross-sectional area of the incoming flow. Stagnation pressures were calculated using the known mean velocity and converting it entirely to pressure.

In addition to the methods described above, we also used a 2-dimensional particle image velocimetry (PIV) system manufactured by DANTEC Dynamics to extract information about the velocity fields in and around the joint/crack for certain test configurations. PIV is a nonintrusive laser optical measurement technique that captures whole-flow-field instantaneous velocity vector measurements in a cross section of the flow. Two velocity components are measured in a plane as a pulsed laser sheet illuminates the field of interest. In our model, the laser sheet entered the test section from above through an acrylic window along the centerline of the test section, allowing streamwise and vertical velocities to be captured, most importantly in the area of the offset and joint/crack. A single digital camera provided these two velocity components. Figure 8 shows a general overview of how a PIV system works.

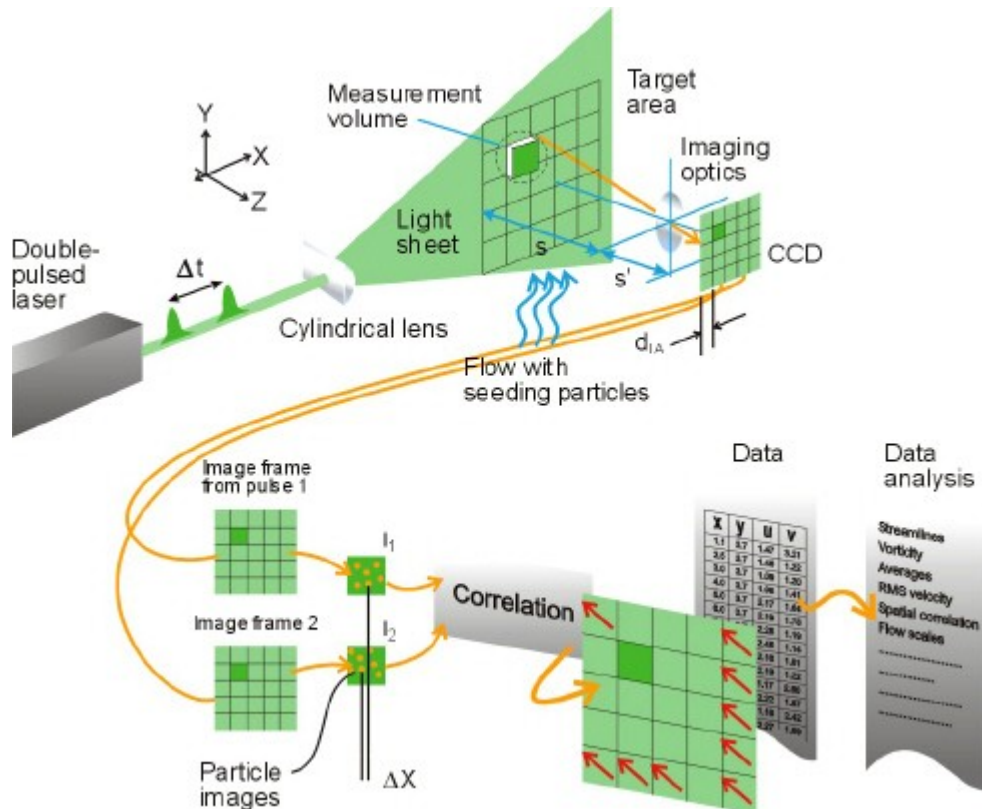


Figure 8.—Overview of the workings of a PIV system. Image courtesy of Dantec.

Two different joint/crack configurations were investigated including 1/2-inch chamfered offsets for the 1/8-inch and 1/2-inch gaps during vented and sealed cavity operation. Free-stream test velocities of 20 ft/s and 30 ft/s were selected for each configuration.

Successive image pairs of the laser-illuminated flow field obtained during testing were processed (cross correlation) to obtain the velocity vector fields. The scale factors obtained from the camera setup were 8.020 and 8.231 pixels/mm for the 1/2-inch and 1/8-inch gap configurations, respectively. External seeding was not required since existing particulates in the laboratory supply system provided decent tracer particle image quality. The time difference between image pairs was set at 50 μ s, the value observed to produce the best cross-correlation results, based on preliminary PIV setup testing over a range of Δt between 25-150 μ s.

The cross correlation process involved 16-pixel by 16-pixel interrogation windows with 50 percent vertical and horizontal overlapping, Gaussian windowing, a No DC filter function. Masking of no-flow zones in the images' field of view was implemented prior to image processing. Figure 9 shows a typical masked image obtained during testing. It was not possible to obtain velocity vector data in the cavity below the slabs since laser-sheet illumination of the flow field was imparted through the slotted window in the top the test section.

The data processing chain can be summarized as: Masked image pairs \rightarrow cross correlation \rightarrow raw vector field \rightarrow moving average validation \rightarrow results vector field \rightarrow Tecplot data loader \rightarrow vector field plots and velocity profile plots. The *moving average validation* algorithm compares three neighboring vectors from the raw vector field plot. If any vector was found to deviate by more than 10 percent of the average of the three vectors, that vector was replaced by the average. Figure 10 shows a typical results vector field plot following validation. The green vectors represent those that were replaced during the validation process.

Numerical Model

Numerical modeling was performed using FlowScience Flow-3D. This commercially available computational fluid dynamics (CFD) package is a finite difference/volume, free surface, transient flow modeling system that solves the Navier-Stokes equation in three spatial dimensions. The finite difference equations are based on an Eulerian mesh of nonuniform hexahedral (brick-shaped) control volumes using the fractional area/volume (FAVOR) method. Free surfaces and material interfaces are defined by fractional volume-of-fluid (VOF) functions. FLOW-3D uses an orthogonal coordinate system as opposed to a body-fitted system. The problem can be set up with a single mesh block, nested mesh blocks, linked mesh blocks, or a combination. The CFD modeling for this project used one mesh block.

Uplift and Crack Flow Resulting from High Velocity Discharges over Open Offset Joints

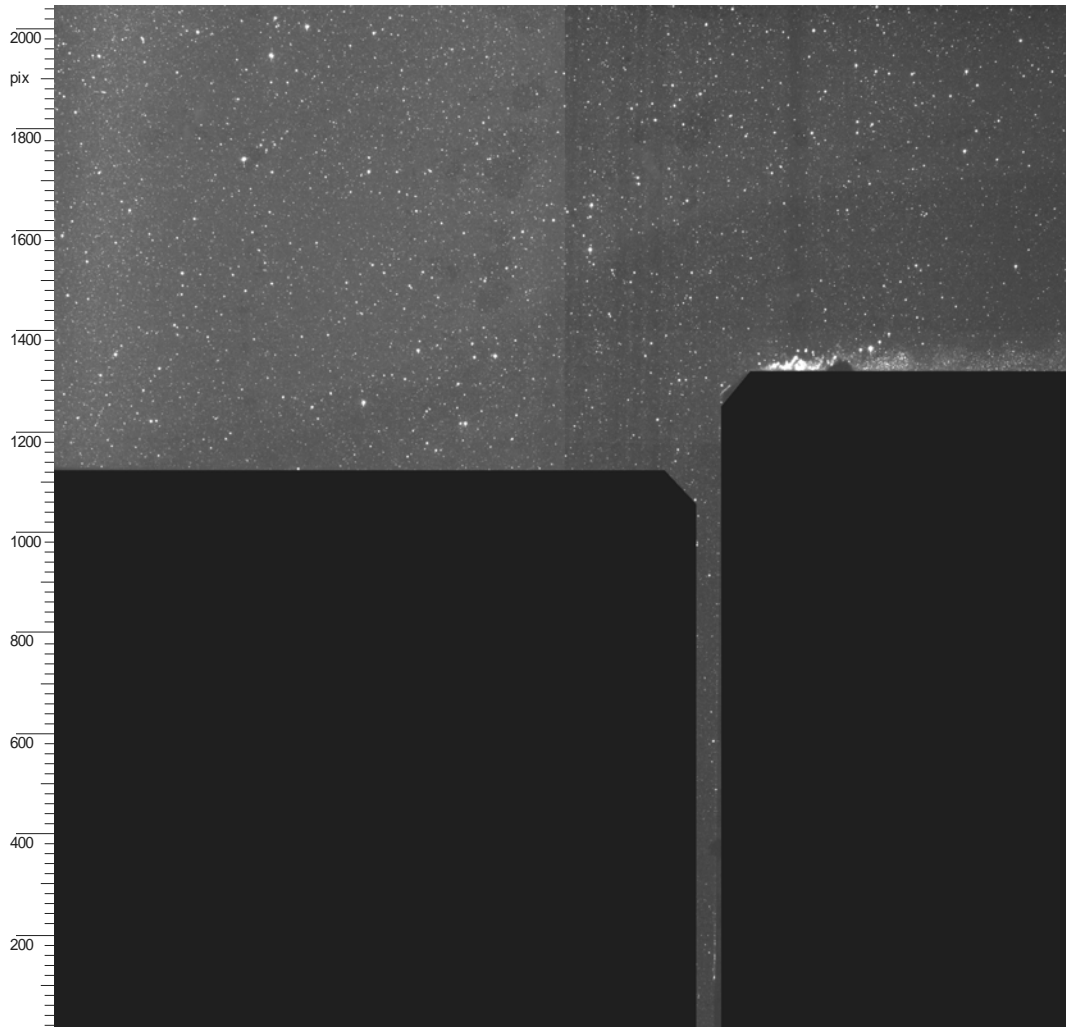


Figure 9.—Typical masked image showing tracer particle density and joint/crack configuration for the ½-inch offset with ⅛-inch gap (flow is left to right).

Model Description

Two numerical models were prepared. One involved simulation of a prototype spillway chute, and the other was a model of the laboratory test section. The size of the time steps greatly influence the computer processing times for these simulations. Finite-difference approximations used to solve time-evolution equations are subject to limits on the size of the time increment. In this type of approximation, it is assumed that the values of all dependent variables are advanced in time through a succession of small time intervals, the time-step. Flow-3D uses a default time-step for stability that limits the convection through every cell to less than 45 percent; velocity and cell size control this. There was minimal definition of the joint/crack (4 cells), and this yielded a time step of about 2.2×10^{-5} seconds. This resulted in more than 3 million cells in the largest of the simulations.

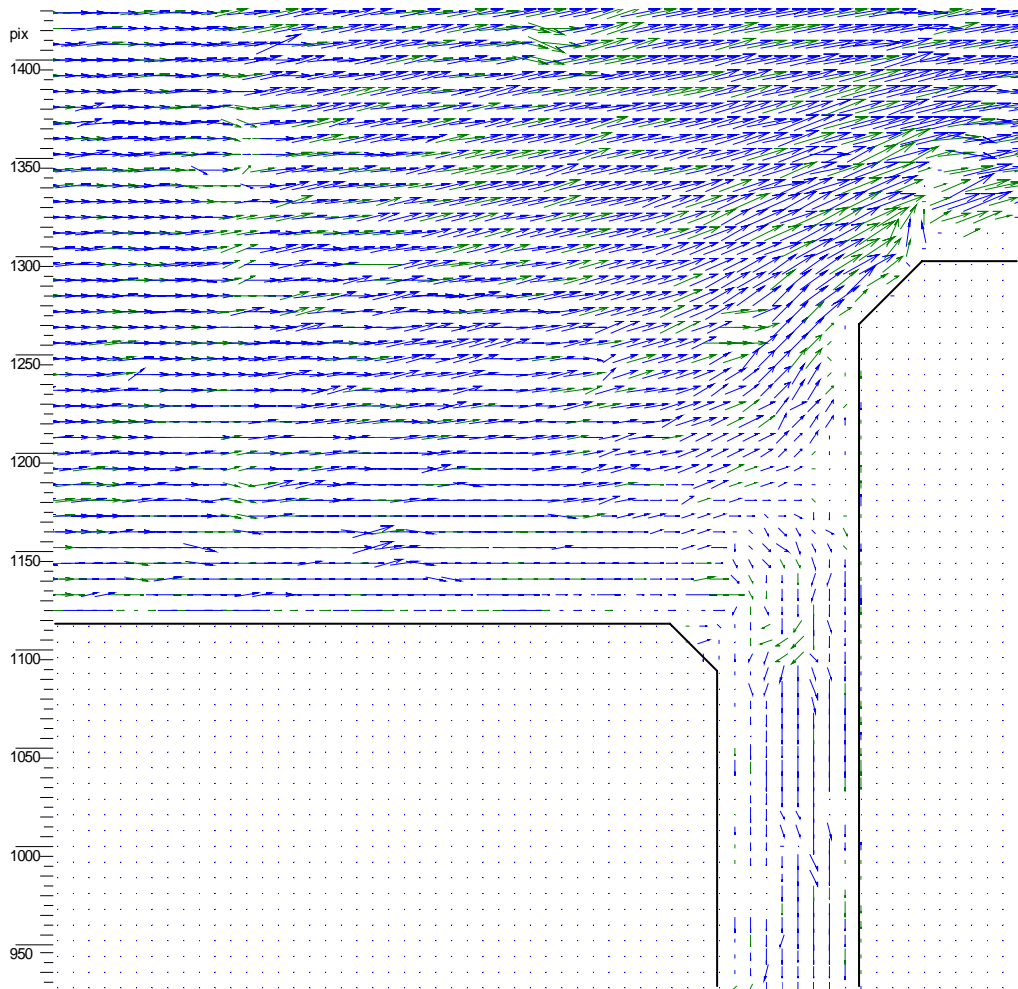


Figure 10.—Typical vector field results following cross-correlation of the masked image pairs and moving average validation for the $\frac{1}{2}$ -inch offset with $\frac{1}{8}$ -inch gap. The green vectors were replaced during the validation process.

Prototype Spillway Chute Simulation

This simulation used a 2-dimensional flow field (oriented in the X-Z plane) with symmetrical boundaries at the minimum and maximum Y plane. The bottom plane of the model was defined as either a no-flow boundary or, when there was flow through the joint/crack, a pressure boundary set at atmospheric pressure. The top boundary was a no-flow boundary.

The upstream and downstream boundaries could not be defined using a standard hydrostatic distribution due to the large velocities considered. Instead, we used a series of small, stacked source obstacles at the upstream end and a series of small, stacked sink obstacles at the downstream end. The magnitudes of the sources and sinks were set to match a modified form of the equation:

$$u = 2.5U \ln \left[\frac{y}{y_0} \right] \quad (1)$$

In this equation, u is the velocity at depth y , y_0 is the total depth, and U is the average velocity. Flow depths of 2, 6, 12, and 24 inches were simulated with a $\frac{1}{8}$ -inch offset into the flow and a $\frac{1}{8}$ -in gap. Boundary conditions were varied to simulate flow entering the joint/crack and seeing atmospheric pressure and also seeing a sealed cavity.

Laboratory Model Simulation

The lab model simulation also used a 2-dimensional flow field but with the planar dimensions similar to those of the model tested in the lab. Basic model definitions were similar to the prototype chute simulation except the inflow boundary was given a constant velocity and allowed to develop for 3 feet prior to the offset/joint combination. The flow and no-flow boundary was treated the same as in the prototype simulation. Two mesh were blocks used. Block 1 used a cell size of 0.06 inches by 0.06 inches, and extended over the first 2 feet of the simulation. Block 2 also was 2 feet in length and featured the offset and joint/crack details with a smaller cell size of 0.03 by 0.03 inches to improve spatial resolution in the vicinity of the joint/crack. The slabs were 4 inches thick and the flow depth was 2 inches. Several offset heights and joint gaps were tested.

Results

The results of these studies have been split into three sections: laboratory model data for uplift pressures and joint/crack flows, supporting lab work using PIV, and numerical modeling using Flow-3D.

Laboratory Model

Three different joint configurations were studied in the laboratory model: sharp-edged, chamfer-edged, and radius-edged. The chamfer and radius were both $\frac{1}{8}$ inch. In all cases, joint/crack gaps were $\frac{1}{8}$, $\frac{1}{4}$, and $\frac{1}{2}$ inch, with offsets into the flow of $\frac{1}{8}$, $\frac{1}{4}$, $\frac{1}{2}$, and $\frac{3}{4}$ inch. The first series of test data presented are for joint/crack orientation perpendicular (90 degrees) to the flow direction.

Sharp-Edged Crack

Pressure and flow rate data were collected according to the process described in the methods section. The data are presented in graphical form as uplift pressure and unit discharge versus velocity with equations for best-fit curves appearing in associated tables.

Data for the 1/8-inch joint/crack gap with sealed lower cavity are presented in figure 11. Uplift pressure versus flow velocity for the case of flow through the joint/crack is shown in figure 12. Lines through the data are best fit power curves and the corresponding equations appear in table 1. The bold upper line represents the stagnation pressure calculated from dynamic pressure $P_d = \rho U^2/2$ where ρ is the density of water and U is the mean flow velocity. P_d is the maximum pressure that is physically possible. Unit joint/crack discharge for the drain configuration modeled is shown on figure 13.

Data for the case of a 1/4-inch joint/crack gap with sealed lower cavity are presented in figure 14. Uplift pressure versus flow velocity for the case of flow through the joint/crack is shown in figure 15. Unit joint/crack discharge for the drain configuration modeled is shown on figure 16.

Data for the case of a 1/2-inch joint/crack gap with sealed lower cavity are presented in figure 17. Uplift pressure versus flow velocity for the case of flow through the joint/crack is shown in figure 18. Unit joint/crack discharge for the drain configuration modeled is shown on figure 19.

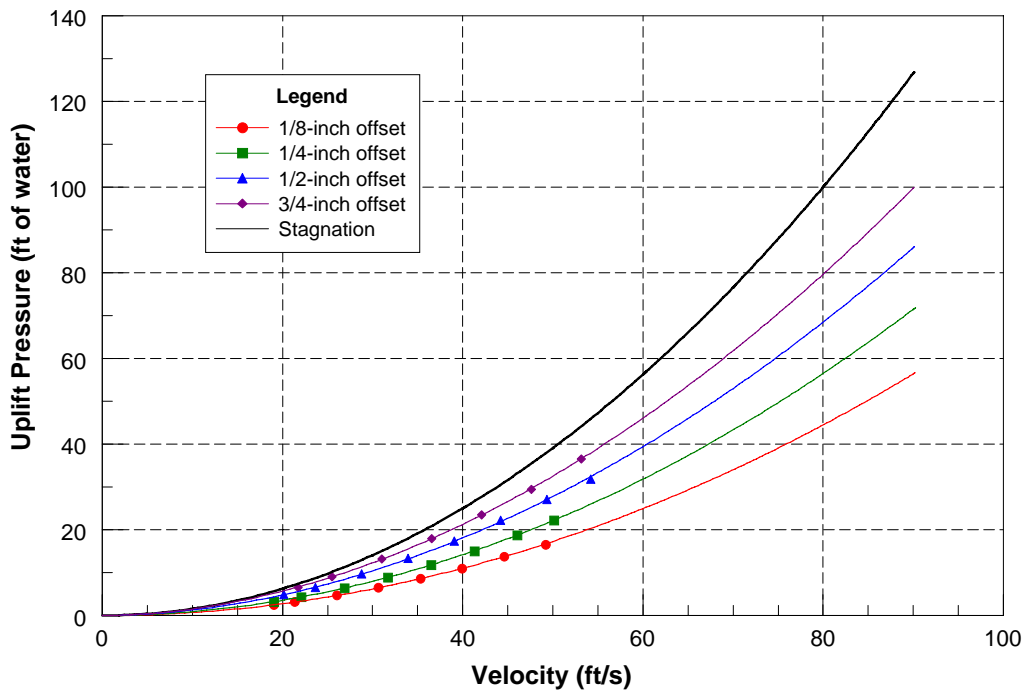


Figure 11.—Mean uplift pressure, sharp-edged geometry, sealed cavity, 1/8-inch gap.

Uplift and Crack Flow Resulting from
High Velocity Discharges over Open Offset Joints

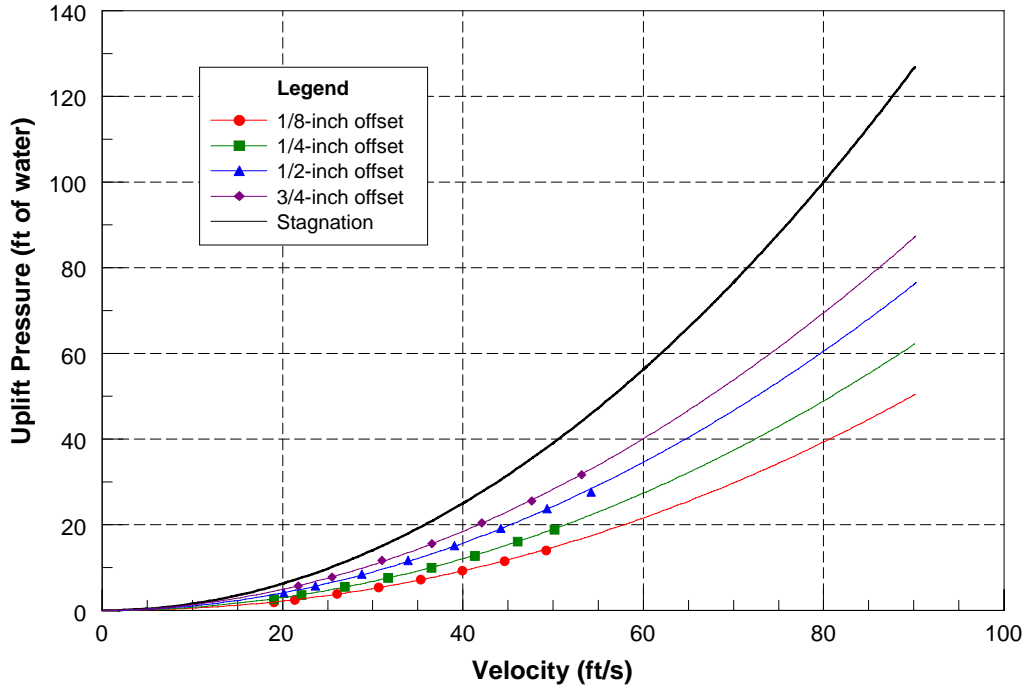


Figure 12.—Mean uplift pressure, sharp-edged geometry, vented cavity, 1/8-inch gap.

Table 1.—Coefficients of power curve fits for sharp-edged geometry. Equation is in the form $P = a U^b$, where U is the velocity and P is the uplift pressure (sealed or vented).

Gap (in)	Offset (in)	Sealed		Vented	
		a	b	a	b
0.125	0.125	0.00659	2.01212	0.00422	2.08575
	0.25	0.00897	1.99619	0.00707	2.01796
	0.50	0.01519	1.92002	0.01207	1.94415
	0.75	0.01881	1.90587	0.01599	1.91156
0.25	0.125	0.00410	2.07475	0.00308	2.11373
	0.25	0.00632	2.06971	0.00546	2.08292
	0.50	0.01055	2.01044	0.00994	2.00543
	0.75	0.01023	2.06377	0.00973	2.05841
0.50	0.125	0.00316	2.04049	0.00243	2.07779
	0.25	0.00500	2.06108	0.00420	2.08693
	0.50	0.00931	2.01530	0.00732	2.06328
	0.75	0.00948	2.07542	0.00909	2.07265

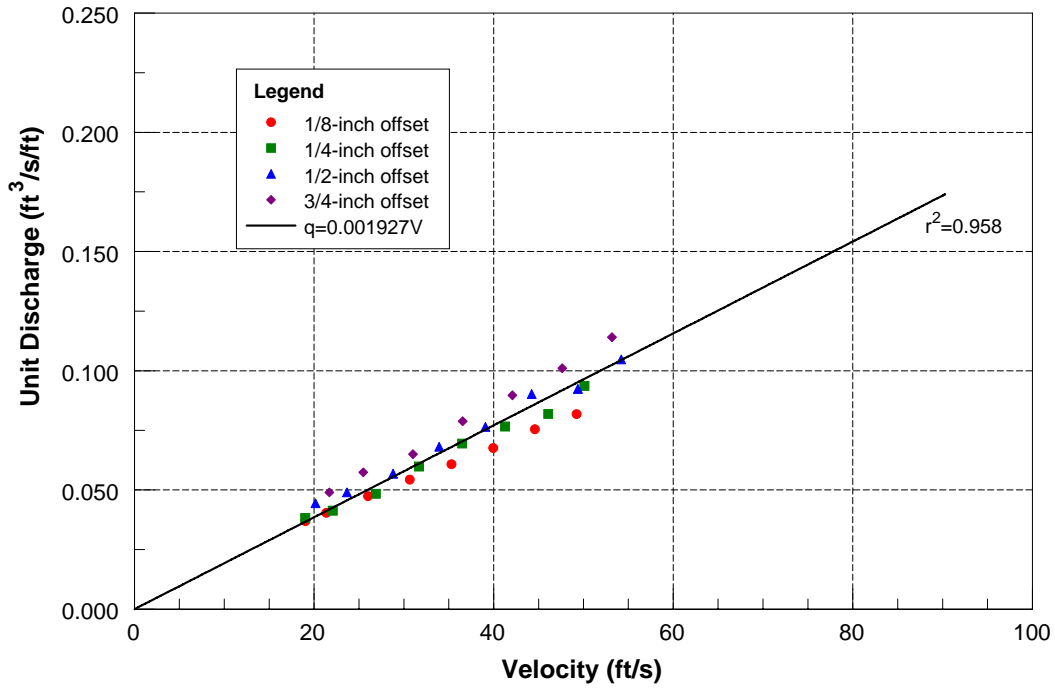


Figure 13.—Unit discharge for joint/crack, sharp-edged geometry, 1/8-inch gap.

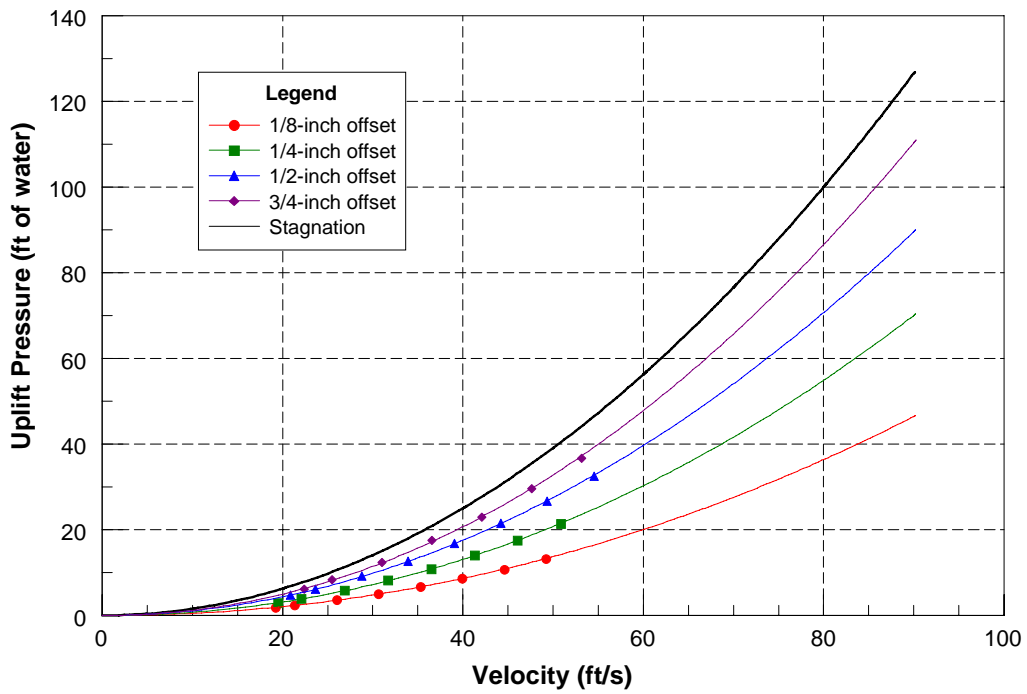


Figure 14.—Mean uplift pressure, sharp-edged geometry, sealed cavity, 1/4-inch gap.

Uplift and Crack Flow Resulting from
High Velocity Discharges over Open Offset Joints

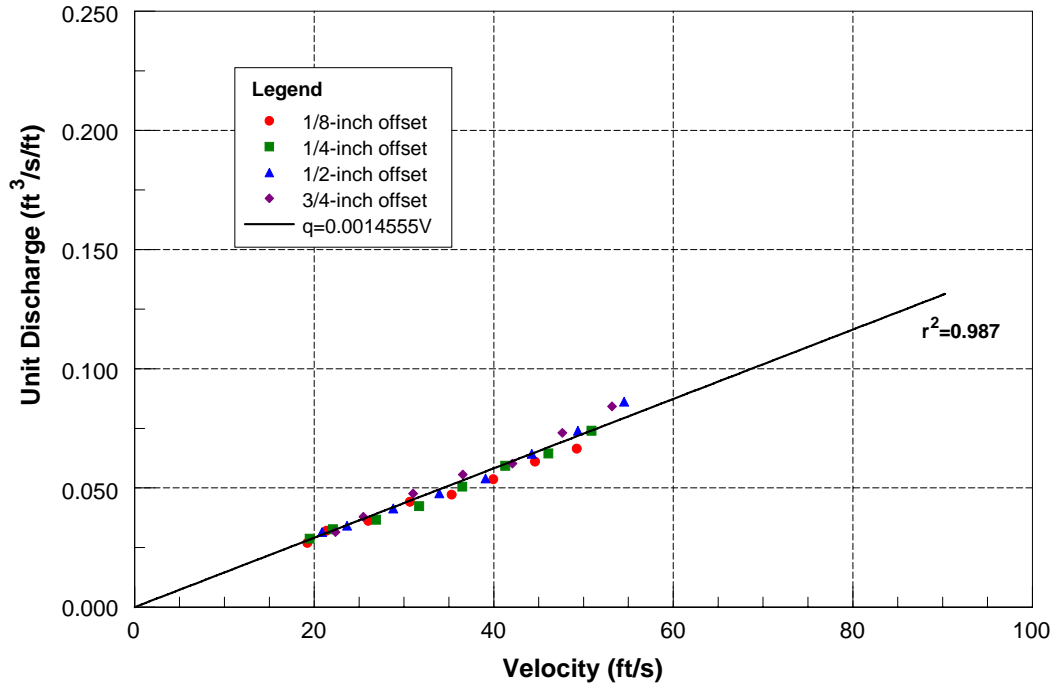


Figure 15.—Mean uplift pressure, sharp-edged geometry, vented cavity, ¼-inch gap.

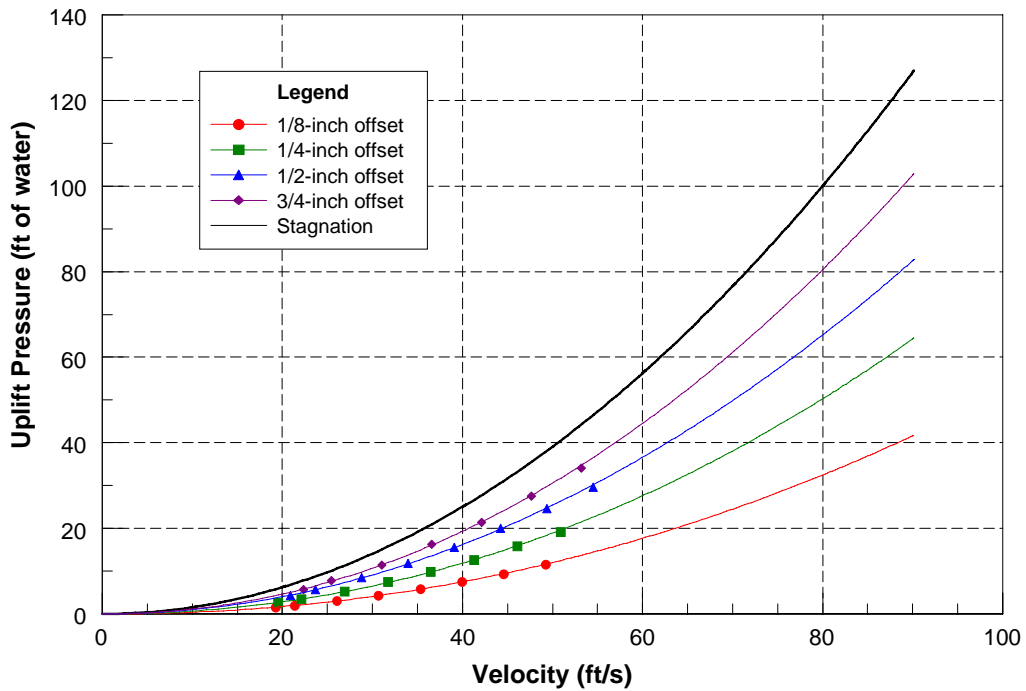


Figure 16.—Unit discharge for sharp-edged joint/crack, ¼-inch gap.

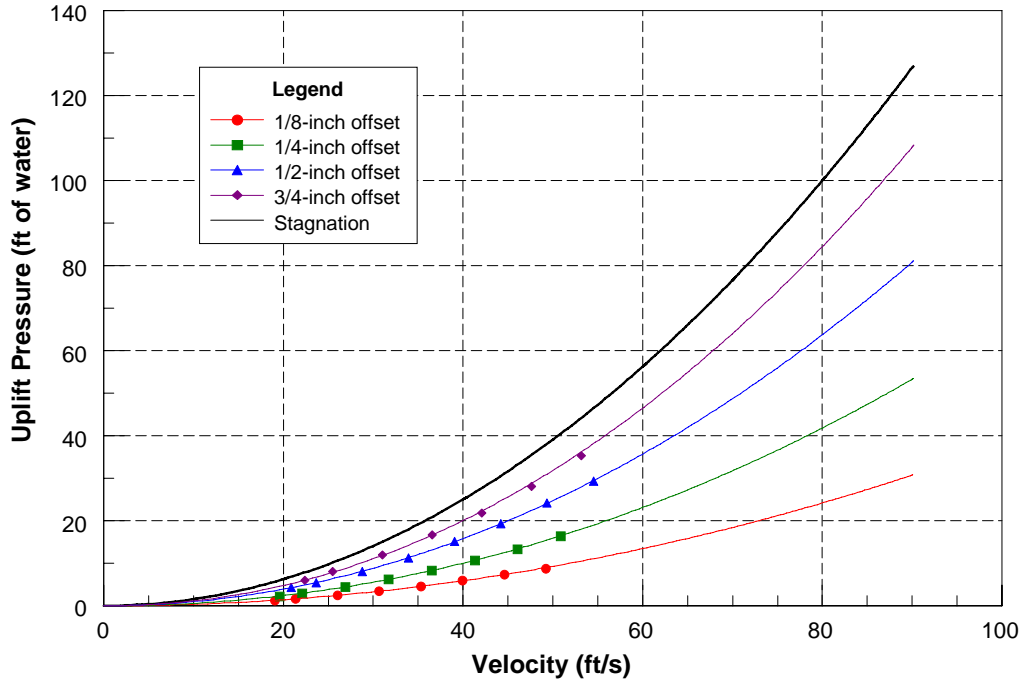


Figure 17.—Mean uplift pressure, sharp-edged geometry, sealed cavity, 1/2-inch gap.

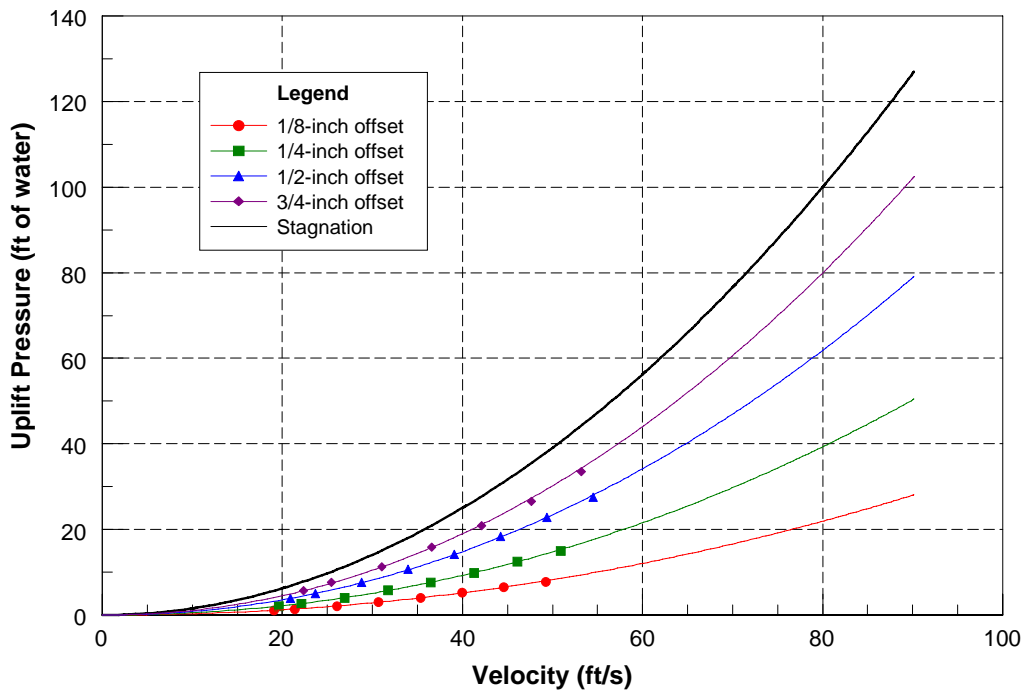


Figure 18.—Mean uplift pressure, sharp-edged geometry, vented cavity, 1/2-inch gap.

Uplift and Crack Flow Resulting from High Velocity Discharges over Open Offset Joints

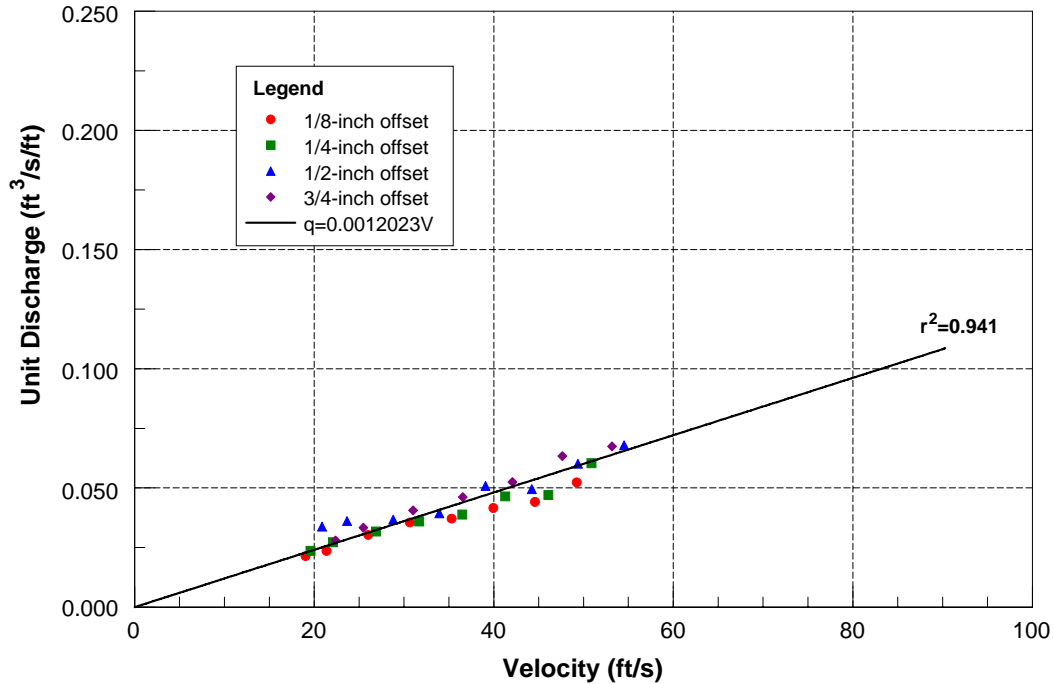


Figure 19.—Unit discharge for sharp-edged joint/crack, 1/2-inch gap.

Chamfer-Edged Crack

The next joint/crack detail that was tested was a chamfer-edged geometry. There were 1/8-inch chamfers on both the leading and trailing edges of the joint/crack. Data for the case of a 1/8-inch joint/crack gap with sealed lower cavity are presented in figure 20. Uplift pressure versus flow velocity for the case of flow through the joint/crack is shown in figure 21. Unit joint/crack discharge for the drain configuration modeled is shown on figure 22. Lines through the data are best-fit power curves and appear in table 2.

Data for the case of a 1/4-inch joint/crack gap with sealed lower cavity are presented in figure 23. Uplift pressure versus flow velocity for the case of flow through the joint/crack is shown in figure 24. Unit joint/crack discharge for the drain configuration modeled is shown on figure 25.

Data for the case of a 1/2-inch joint/crack gap with sealed lower cavity are presented in figure 26. Uplift pressure versus flow velocity for the case of flow through the joint/crack is shown in figure 27. Unit joint/crack discharge for the drain configuration modeled is shown on figure 28.

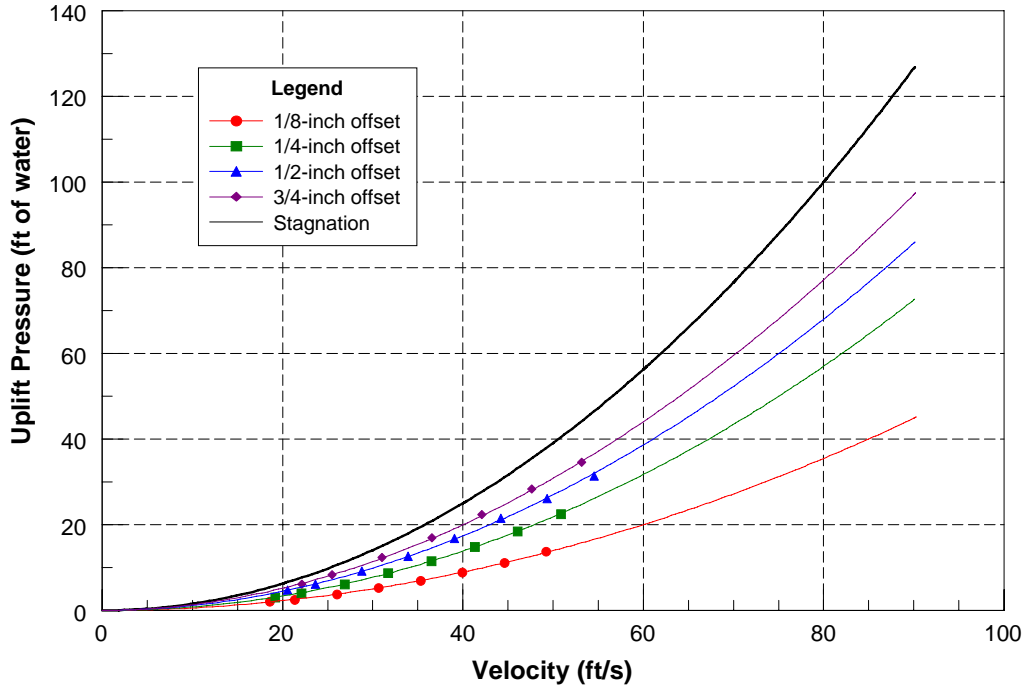


Figure 20.—Mean uplift pressure, chamfer-edged geometry, sealed cavity, 1/8-inch gap.

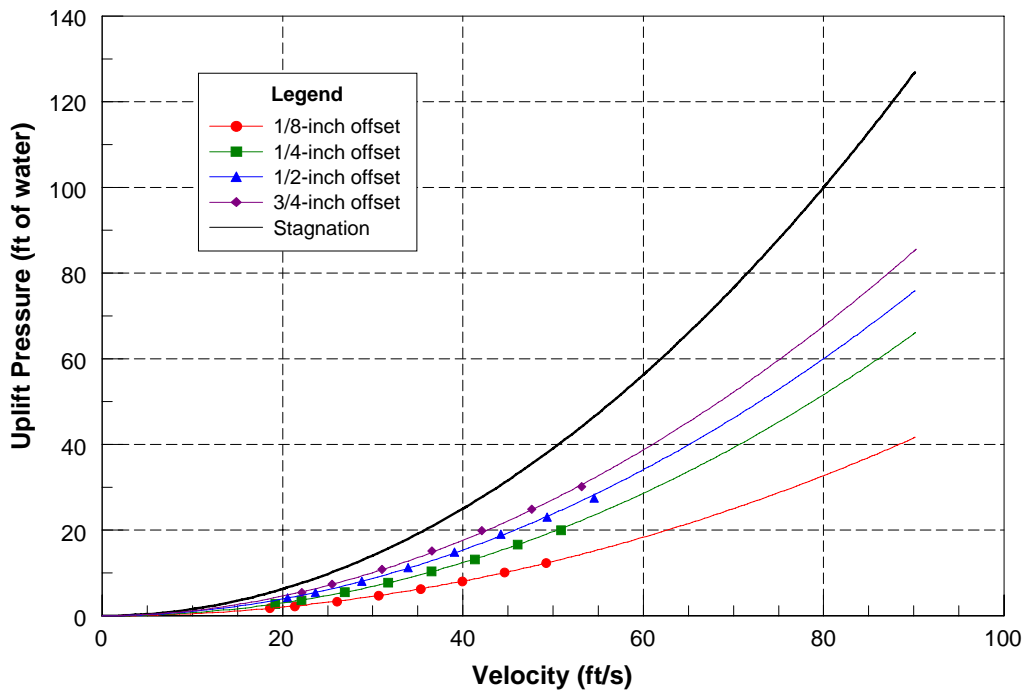


Figure 21.—Mean uplift pressure, chamfer-edged geometry, vented cavity, 1/8-inch gap.

Uplift and Crack Flow Resulting from
High Velocity Discharges over Open Offset Joints

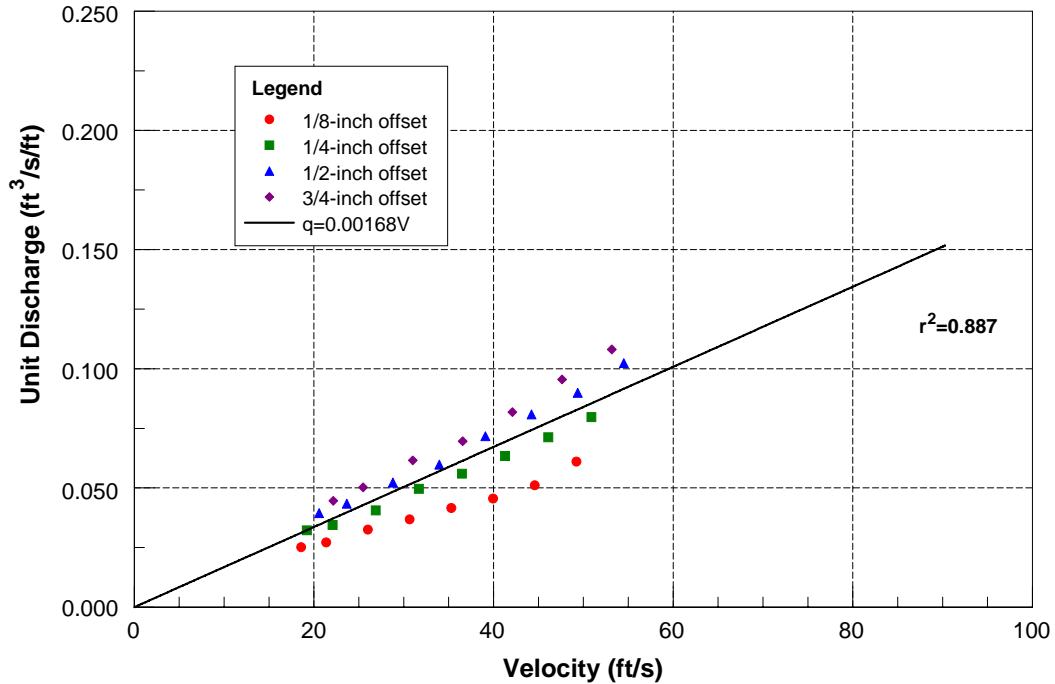


Figure 22.—Unit discharge into gap, chamfer-edged geometry, 1/8-inch gap.

Table 2.—Coefficients of power curve fits for chamfer-edged geometry. Equation is in the form $P = a U^b$, where U is the velocity and P is the uplift pressure (sealed or vented)

Gap (in)	Offset (in)	Sealed		Vented	
		a	b	a	b
0.125	0.125	0.00585	1.98750	0.00477	2.01598
	0.25	0.00749	2.03969	0.00629	2.05685
	0.50	0.01227	1.96715	0.01084	1.96694
	0.75	0.01502	1.94983	0.01355	1.94340
0.25	0.125	0.00417	1.99452	0.00316	2.03835
	0.25	0.00688	2.01279	0.00585	2.03202
	0.50	0.01037	2.00675	0.01019	1.99466
	0.75	0.01151	2.01853	0.01125	2.00847
0.50	0.125	0.00381	1.94684	0.00243	2.03809
	0.25	0.00575	1.99605	0.00478	2.02460
	0.50	0.00961	1.98766	0.00879	1.99484
	0.75	0.01121	2.00462	0.01056	2.00565

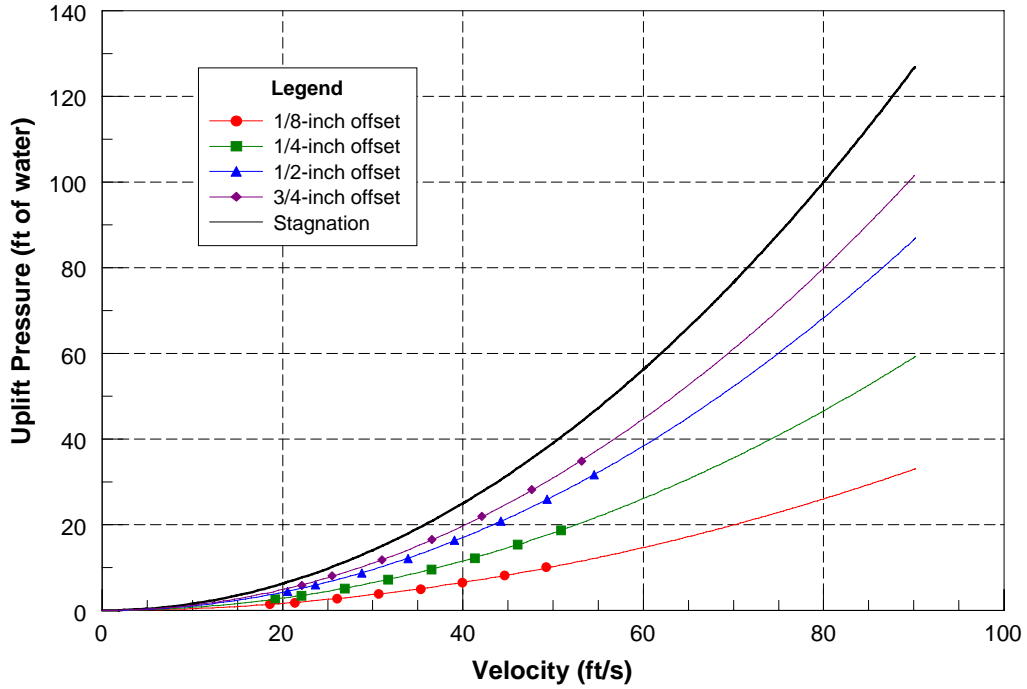


Figure 23.—Mean uplift pressure, chamfer-edged geometry, sealed cavity, 1/4-inch gap.

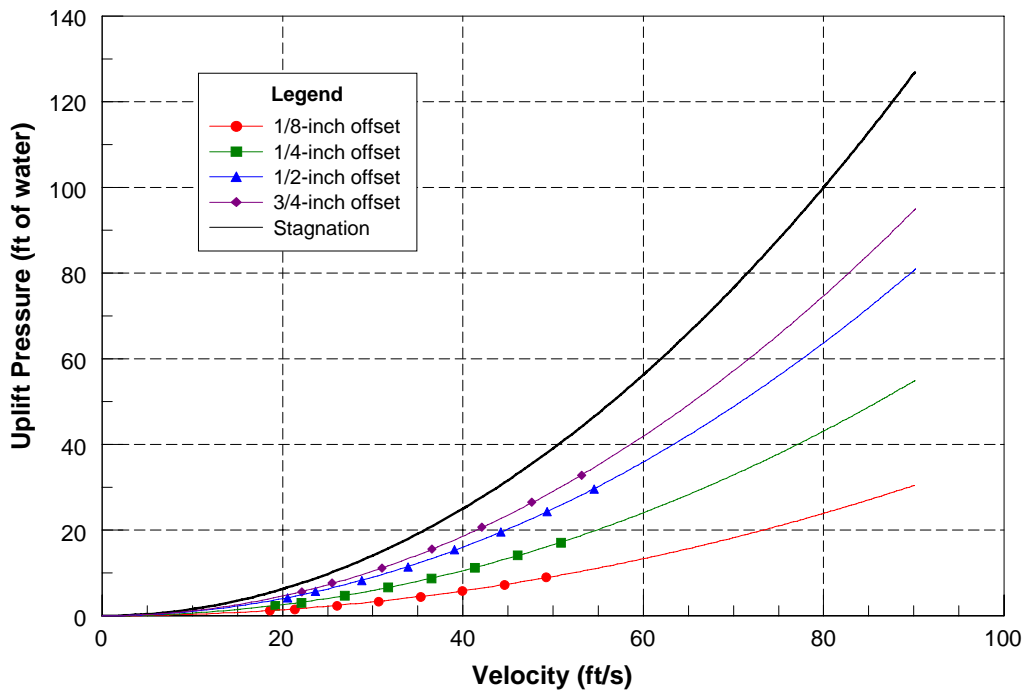


Figure 24.—Mean uplift pressure, chamfer-edged geometry, vented cavity, 1/4-inch gap.

Uplift and Crack Flow Resulting from High Velocity Discharges over Open Offset Joints

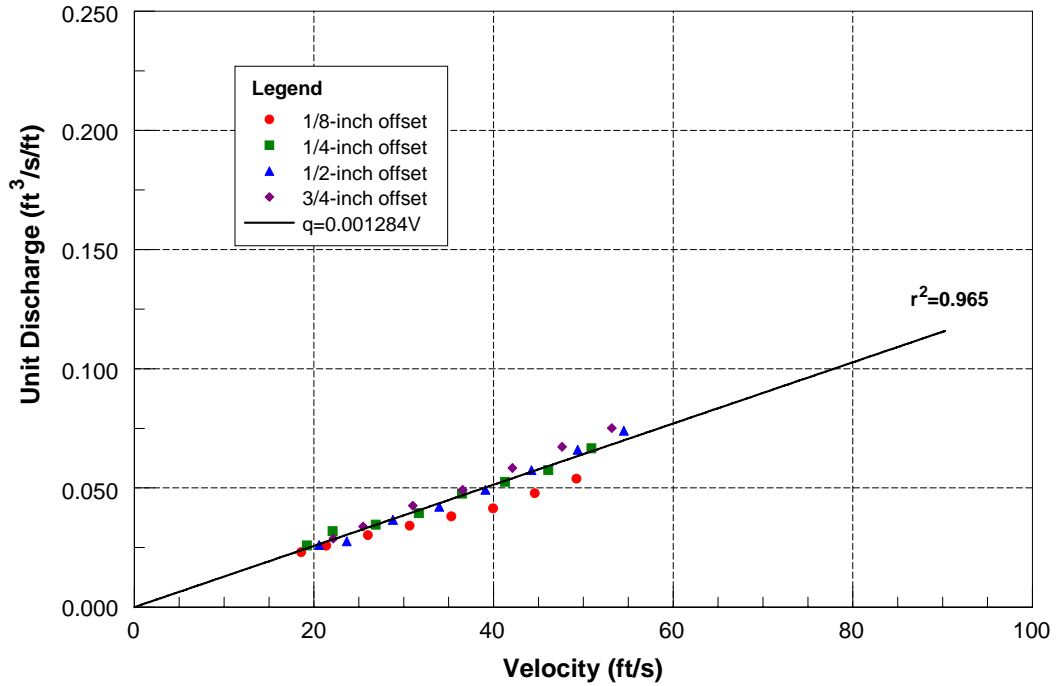


Figure 25.—Unit discharge through joint/crack, chamfer-edged, ¼-inch gap.

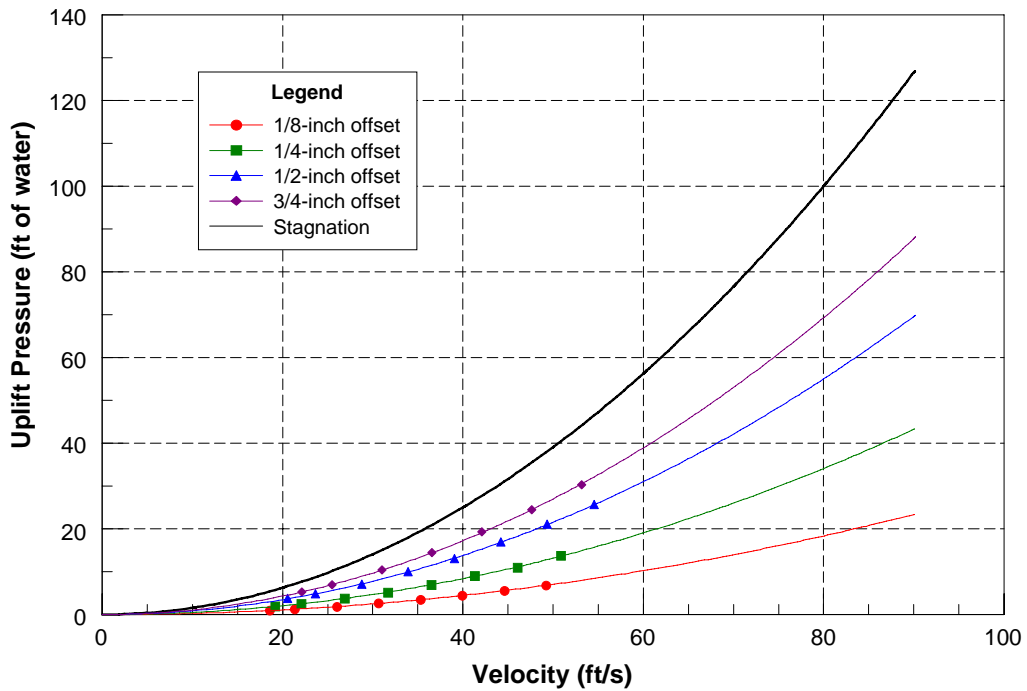


Figure 26.—Mean uplift pressure, chamfer-edged geometry, sealed cavity, ½-inch gap.

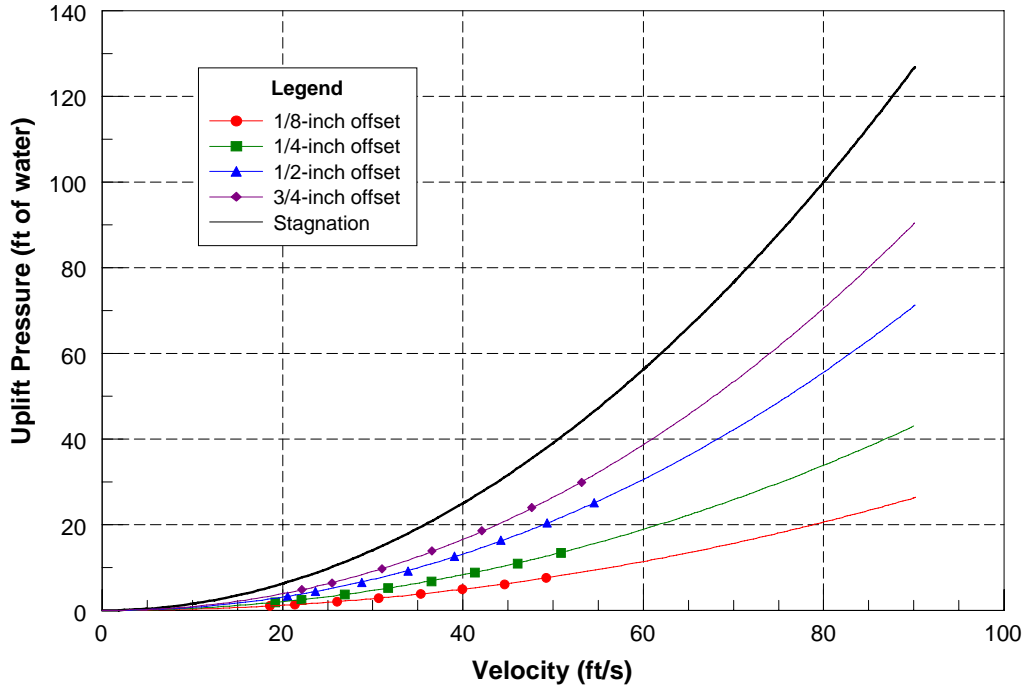


Figure 27.—Mean uplift pressure, chamfer-edged geometry, vented cavity, 1/2-inch gap.

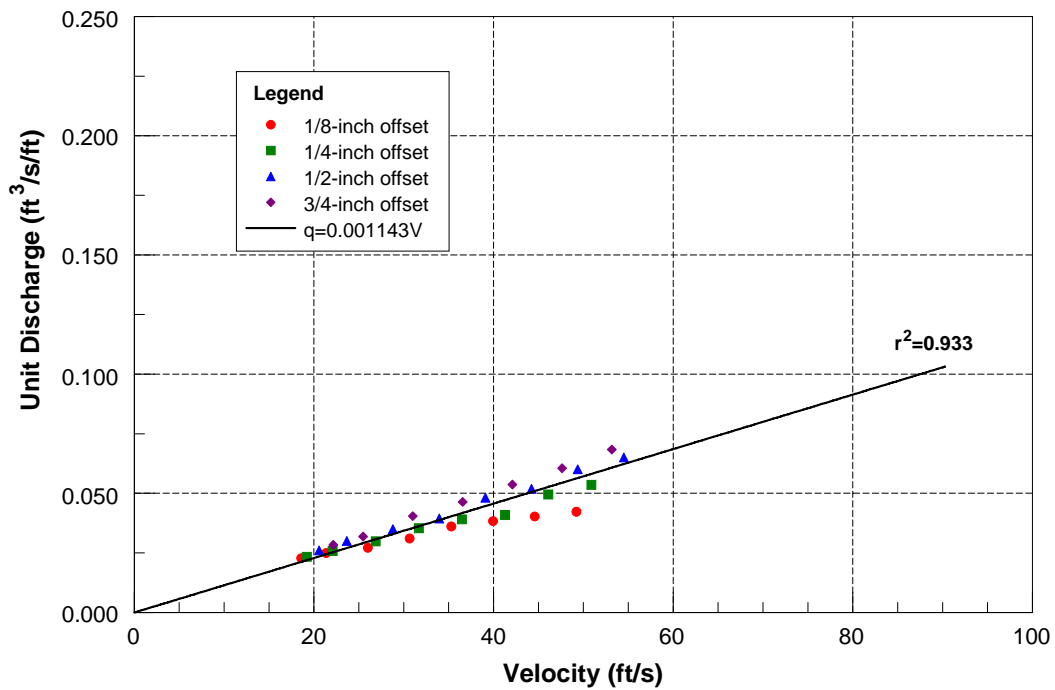


Figure 28.—Unit discharge through joint/crack, chamfer-edged, 1/2-inch gap.

Radius-Edged Crack

The next joint/crack detail that was tested was a radius-edged geometry. There were $\frac{1}{8}$ -inch radii on both the leading and trailing edges of the joint/crack. Data for the case of a $\frac{1}{8}$ -inch joint/crack gap with sealed lower cavity are presented in figure 29. Uplift pressure versus flow velocity for the case of flow through the joint/crack is shown in figure 30. Unit joint/crack discharge for the drain configuration modeled is shown on figure 31. Lines through the data are best-fit power curves, and the coefficients appear in table 3.

Data for the case of a $\frac{1}{4}$ -inch joint/crack gap with sealed lower cavity are presented in figure 32. Uplift pressure versus flow velocity for the case of flow through the joint/crack is shown in figure 33. Unit joint/crack discharge for the drain configuration modeled is shown on figure 34.

Data for the case of a $\frac{1}{2}$ -inch joint/crack gap with sealed lower cavity are presented in figure 35. Uplift pressure versus flow velocity for the case of flow through the joint/crack is shown in figure 36. Unit joint/crack discharge for the drain configuration modeled is shown on figure 37.

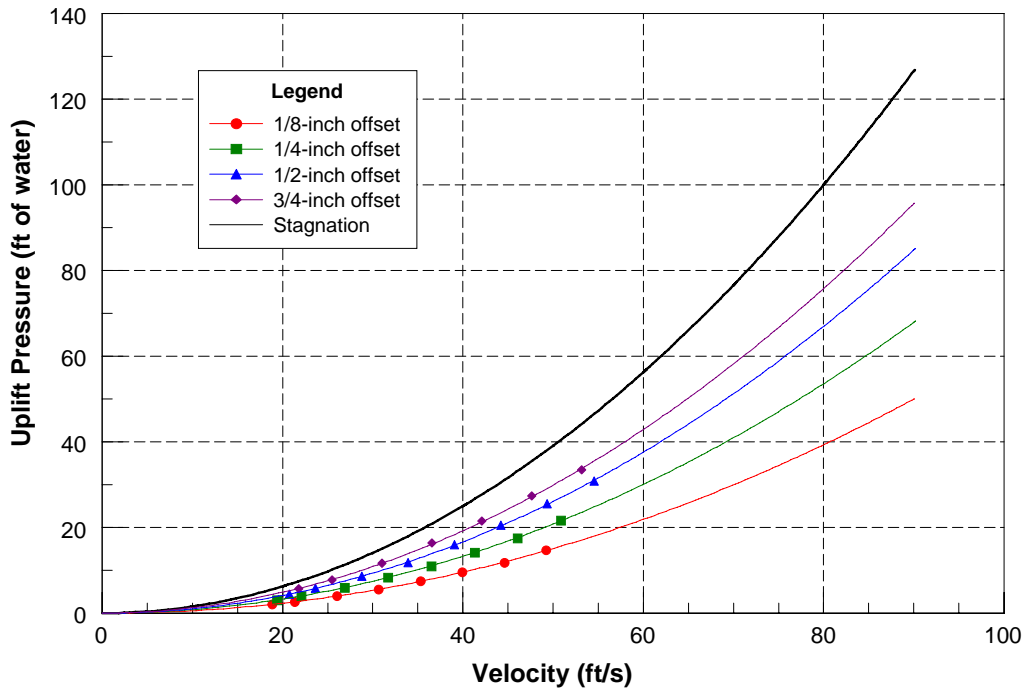


Figure 29.—Mean uplift pressure, radius-edged geometry, sealed cavity, $\frac{1}{8}$ -inch gap.

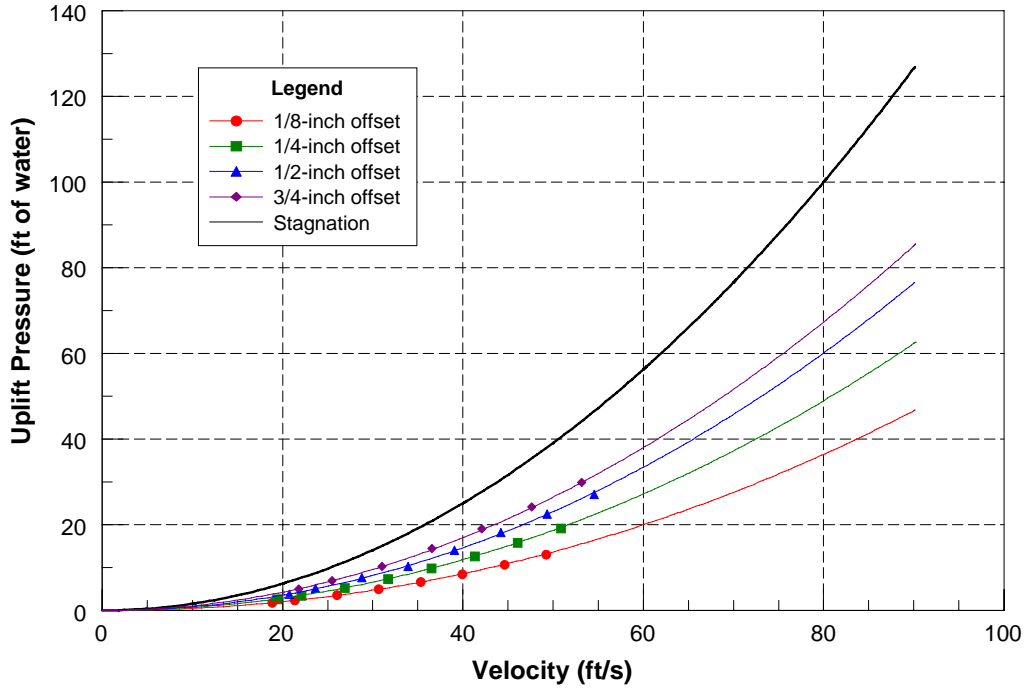


Figure 30.—Mean uplift pressure, radius-edged geometry, vented cavity, 1/8-inch gap.

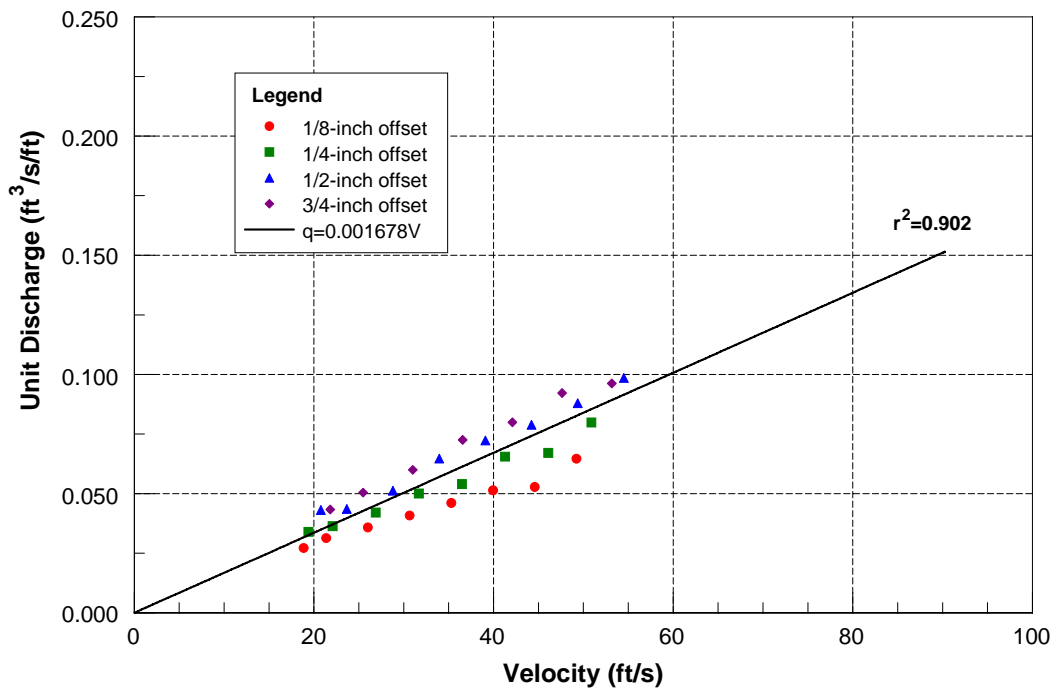


Figure 31.—Unit discharge through joint/crack, radius-edged, 1/8-inch gap.

Uplift and Crack Flow Resulting from
High Velocity Discharges over Open Offset Joints

Table 3.—Coefficients of power curve fits for radius-edged geometry. Equation is in the form $P = a U^b$, where U is the velocity and P is the uplift pressure (sealed or vented)

Gap (in)	Offset (in)	Sealed		Vented	
		a	b	a	b
0.125	0.125	0.00520	2.03812	0.00387	2.08813
	0.25	0.00795	2.01167	0.00622	2.04700
	0.50	0.01012	2.00758	0.00790	2.03953
	0.75	0.01295	1.97952	0.01101	1.98957
0.25	0.125	0.00425	2.00912	0.00333	2.04385
	0.25	0.00687	2.00842	0.00575	2.03262
	0.50	0.00898	2.03395	0.00838	2.03420
	0.75	0.00904	2.07469	0.00869	2.06829
0.50	0.125	0.00344	2.00152	0.00253	2.05472
	0.25	0.00542	2.00793	0.00470	2.02695
	0.50	0.00676	2.06924	0.00614	2.07939
	0.75	0.00785	2.09152	0.00741	2.09057

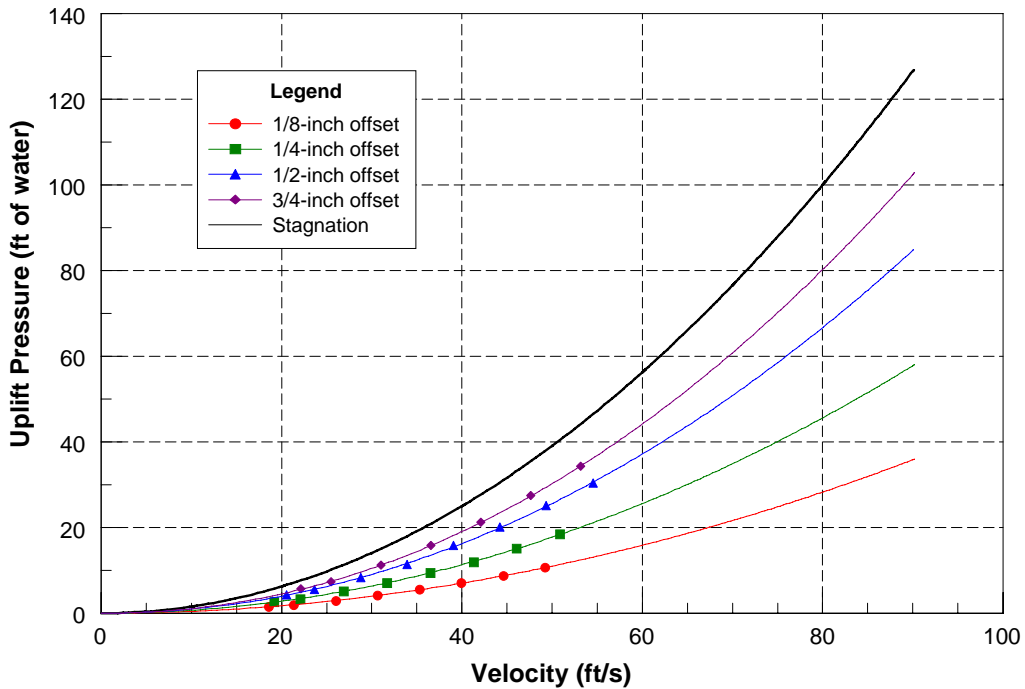


Figure 32.—Mean uplift pressure, radius-edged, sealed cavity, 1/4-inch gap.

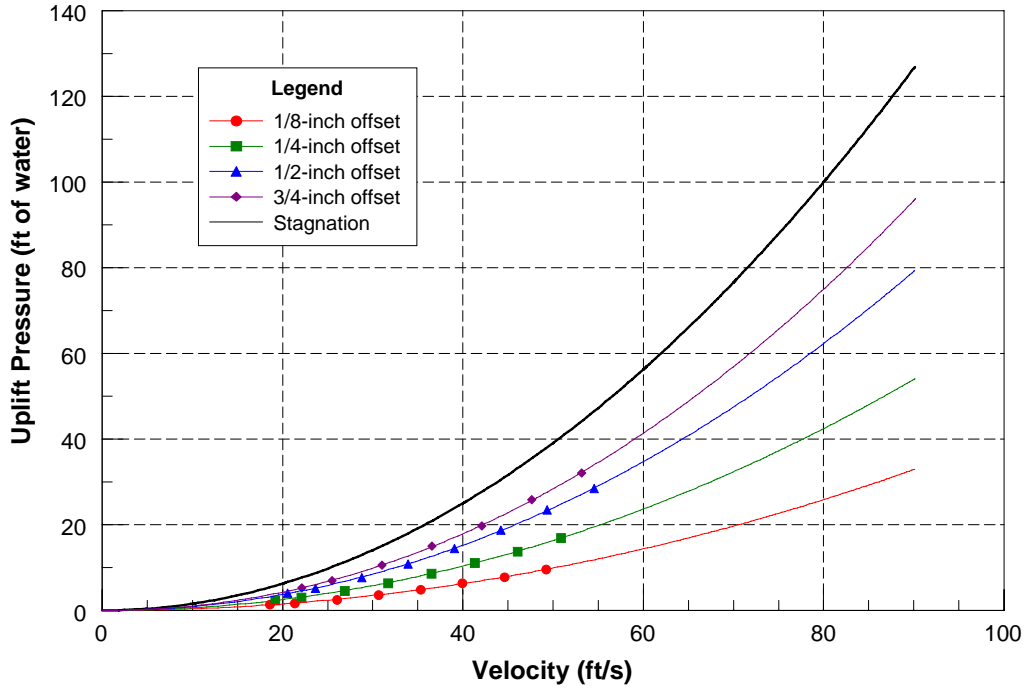


Figure 33.—Mean uplift pressure, radius-edged geometry, vented cavity, 1/4-inch gap.

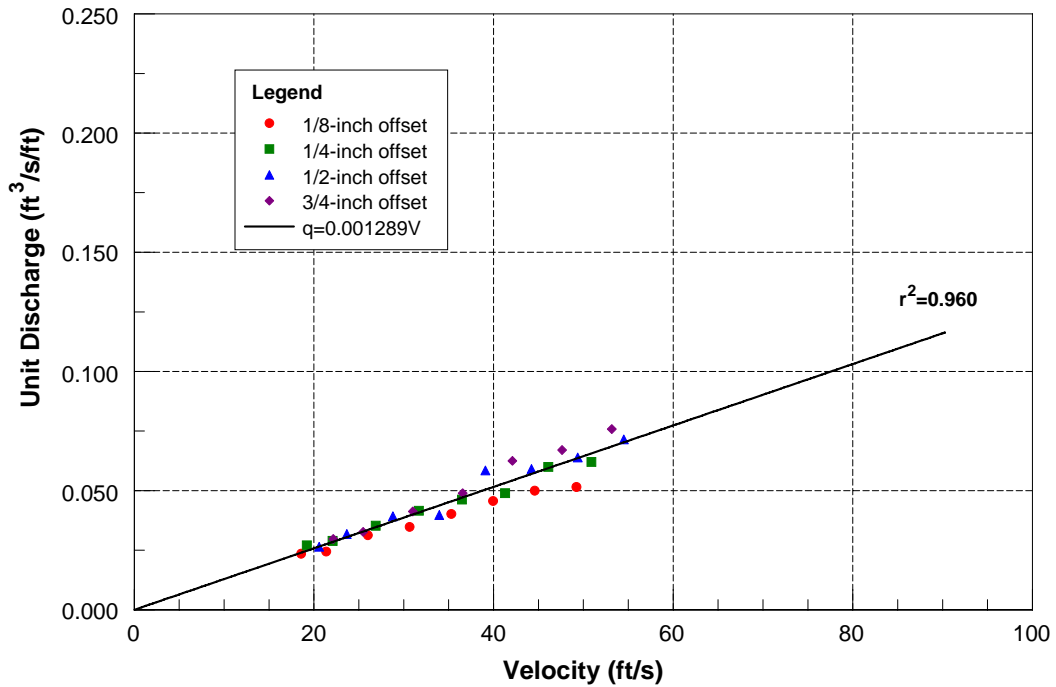


Figure 34.—Unit discharge through joint/crack, radius-edged, 1/4-inch gap.

Uplift and Crack Flow Resulting from
High Velocity Discharges over Open Offset Joints

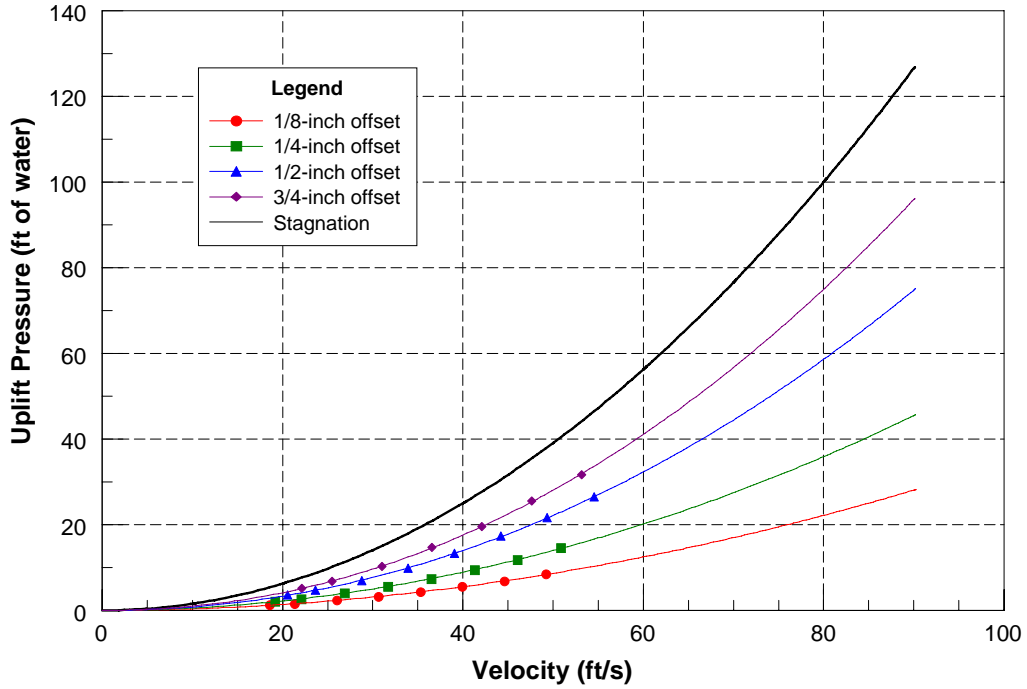


Figure 35.—Mean uplift pressure, radius-edged geometry, sealed cavity, ½-inch gap.

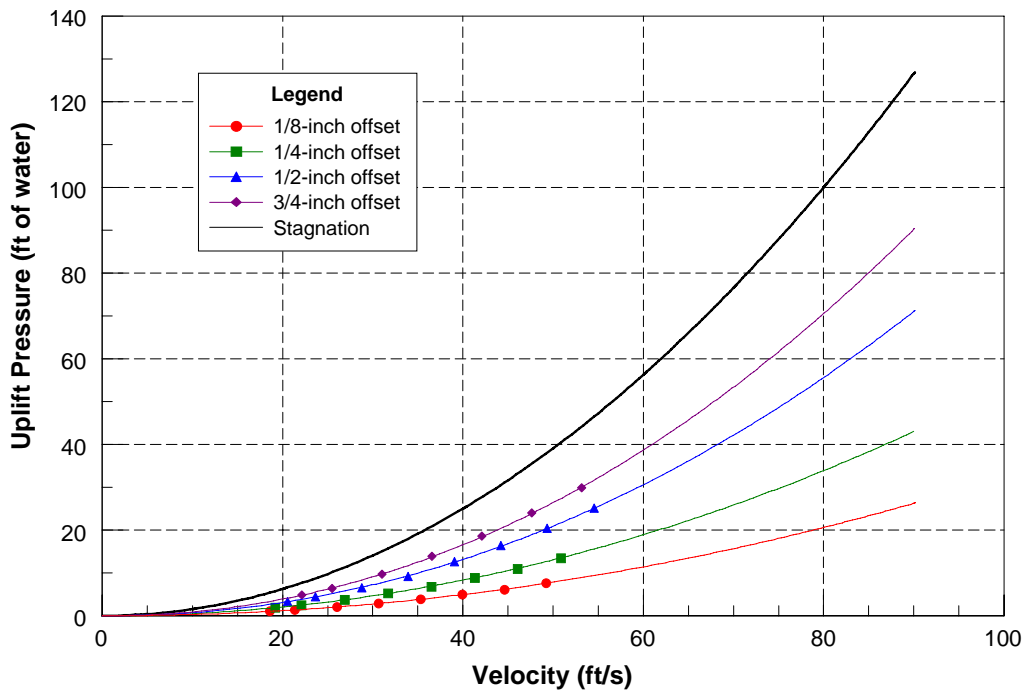


Figure 36.—Mean uplift pressure, radius-edged geometry, vented cavity, ½-inch gap.

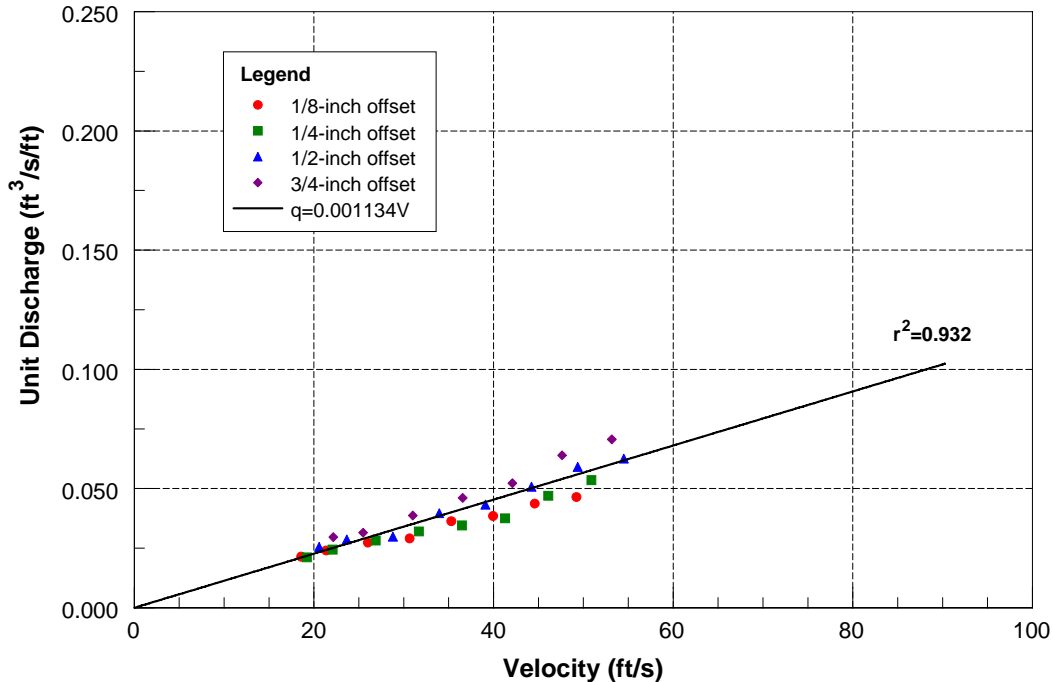


Figure 37.—Unit discharge through joint/crack, radius-edged geometry, 1/2-inch gap.

General Trends

In general, for all cases tested, the uplift pressure increases with increased flow velocity and increased offset height. However, increased joint/crack gaps show slight reductions in uplift pressures. Venting the cavity below also produces a reduction in uplift pressure for all test configurations. Comparisons between the different joint/crack geometries, sharp vs. chamfered vs. radius, yielded a general result that the chamfer and radius edged joint/cracks yielded results of an effectively wider gap compared to the sharp edges. For example, the 1/4-inch wide gap with the sharp edges yielded similar uplift pressure values to those of the 1/8-inch gap for the chamfered and radius edges.

As regards joint/crack unit discharge, the results consistently show that increased joint/crack gaps produce reduced unit discharges for fixed geometry (i.e., sharp-edge, chamfer-edge, or radius-edge), yet the results are only slightly sensitive to offset height, the sensitivity of which slightly increases with reduced joint/crack gap. In comparison of the different geometries, the unit discharge becomes more sensitive to offset height for the chamfer and radius-edged geometries, particularly for small joint/crack gaps. In other words, unit discharge increases significantly with offset height for small joint/crack gaps. In terms of the gap width, unit discharges for all offsets tested tended to collapse on a single line for the widest gap (1/2-inch) and separate to individual lines as the gap decreased. This was especially evident for the chamfered and radius joint/cracks. The straight-edged joint/crack collapsed relatively well for all gaps. These unit discharge data were fit with a single straight line for simplicity in applying the

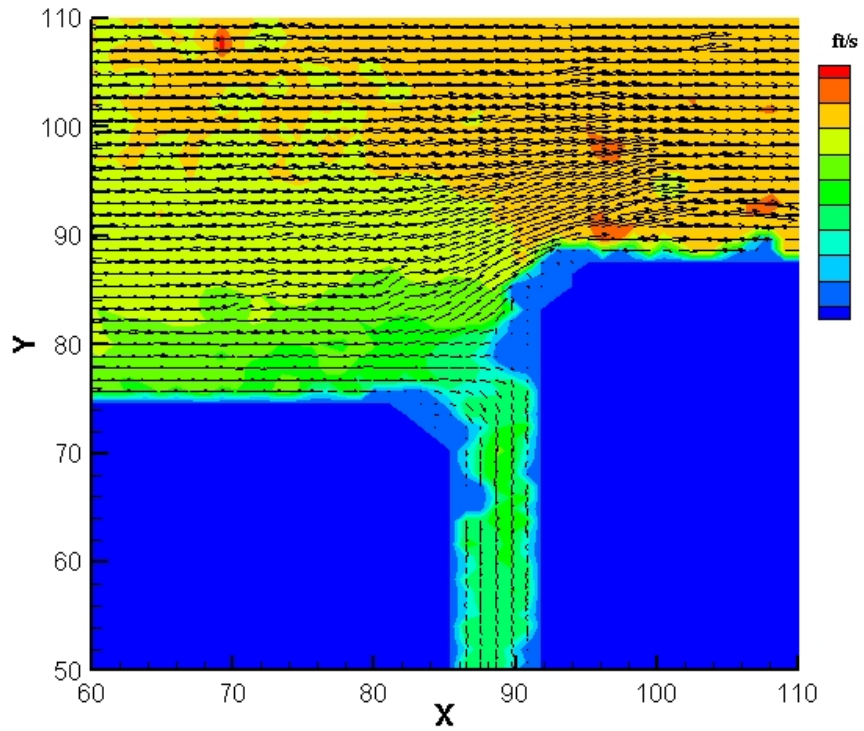
result; however the individual lines representing the various offset heights could easily be provided. In all cases tested, limitations in drain capacity controlled the flow through the gap. This is most likely to be the case in prototype installations as well. The application of basic head loss theory then makes it relatively easy to predict gap flows for a variety of drain-loss configurations. Venting of the subcavity to atmospheric pressure, while unlikely to occur, does produce the highest flows into the gap.

Particle Image Velocity

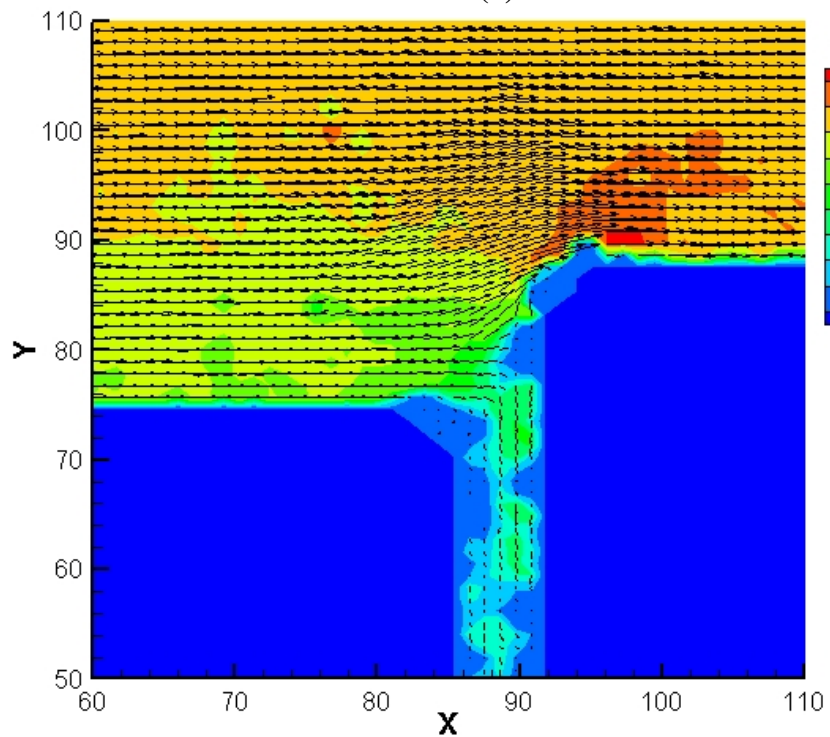
Figures 38 through 41 show the velocity field results obtained for 1/2-inch chamfered offsets with 1/8-inch and 1/2-inch gaps during vented and sealed cavity operation with free-stream test velocities of 20 ft/s and 30 ft/s. The data are presented as resultant velocity vectors overlaying color contour plots of the resultant velocity magnitudes (flow is left to right). The ordinate and abscissa are given as X and Y coordinates of the interrogation windows center points from cross-correlation processing of image pairs.

In general, the results show the effects of gap, venting, and free stream velocity on the flow patterns in the vicinity of the joint/crack and offset for the range of configurations and operating conditions tested. The general effects of venting for all cases tested include: (1) a slight change in the general extent of the stagnation zone near the upstream face of the offset as venting tends to increase the extent in comparison with sealed cavity operation; (2) alteration of the stream lines for the flow passing above the joint/crack as venting tends to reduce the streamline displacement as compared with sealed cavity operation; and (3) increased vertical velocities into the joint/crack due to flow into the vent cavity during vented operation. However, the 1/2-inch gap exhibits greater sensitivity to venting as shown in figures 40 and 41 in comparison with the 1/8-inch gap (figures 38 and 39). This is primarily due to the establishment of a dominant recirculation zone just downstream and below the trailing edge of the upstream slab for the 1/2-inch gap, which is observed for both 20- and 30-ft/s free stream velocities. Such recirculation is not evident for the 1/8-inch gap configuration under these test conditions.

The most interesting feature of the recirculation zone for the 1/2-inch gap involves the *effective width* through which dominant vertical velocities are observed. This *effective width* appears to decrease slightly with increased free-stream velocity. Such a result is physically reasonable in consideration of increased changes in momentum necessary to turn the flow vertically downward for increased free-stream when the possibility for recirculation zone exists. In this regard, it appears that a smaller joint/crack gap is more conducive (at least along the test section centerline and for the free-stream velocities tested) to producing flow through the joint/crack during vented operation because it eliminates or at least limits the extent of recirculation. However, this physical explanation is complicated by the drive pressure presumably transmitted by stagnating flow along the offset face.



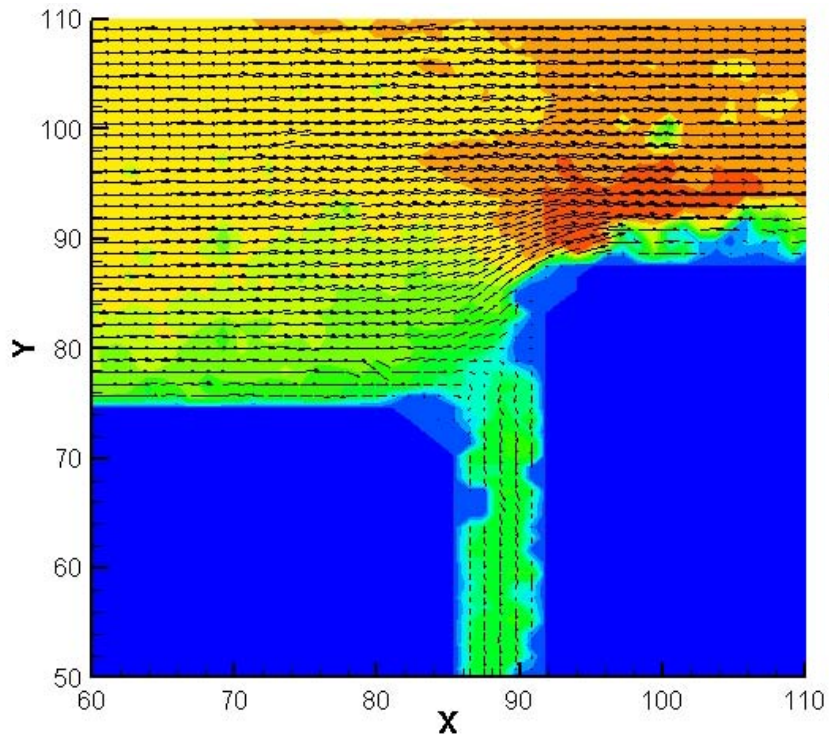
(a)



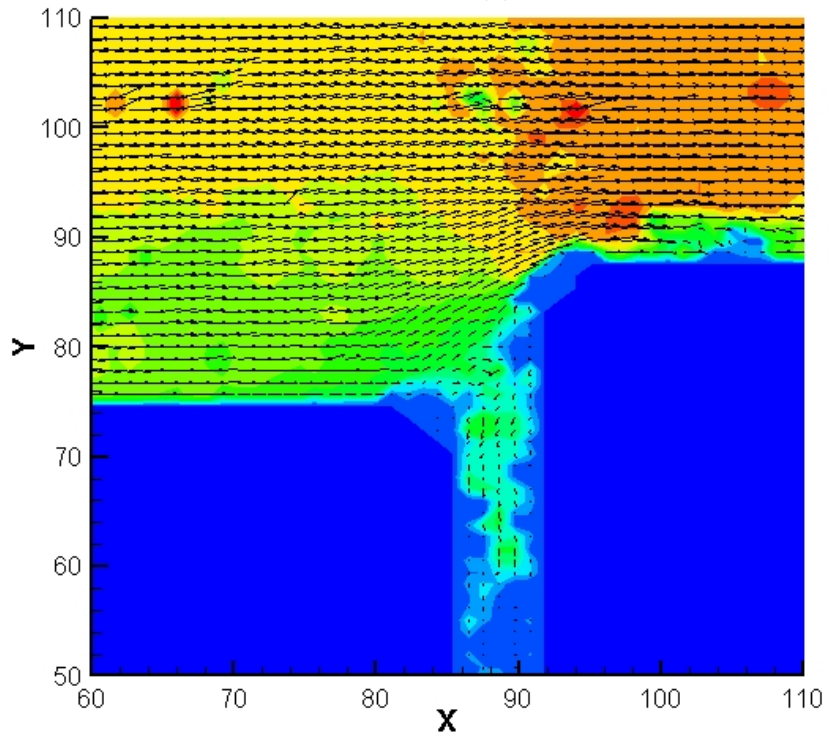
(b)

Figure 38.—Velocity fields for the 1/2-inch gap and 1/2-inch chamfered offset at 20-ft/s free stream velocity test conditions: (a) vented and (b) sealed cavity.

Uplift and Crack Flow Resulting from
High Velocity Discharges over Open Offset Joints

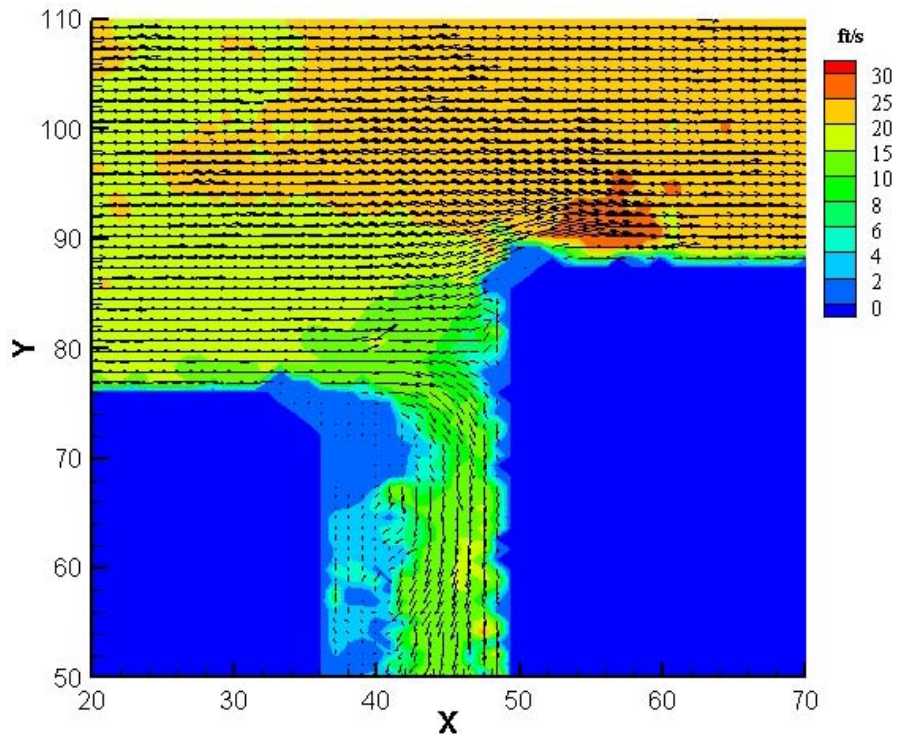


(a)

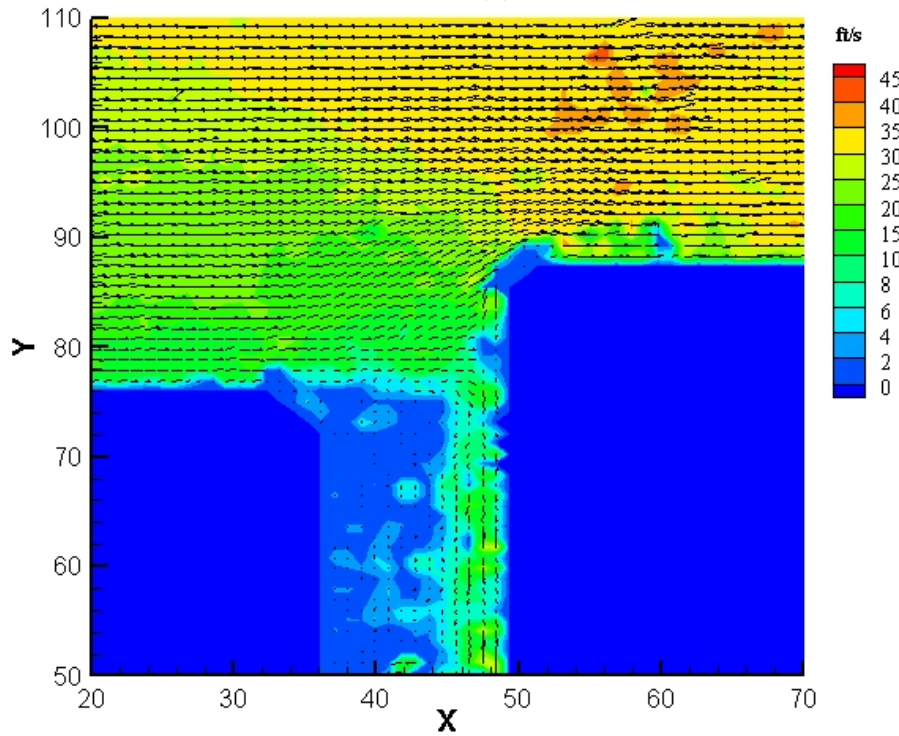


(b)

Figure 39.—Velocity fields for the 1/2-inch gap and 1/2-inch chamfered offset at 30-ft/s free stream velocity test conditions: (a) vented and (b) sealed cavity.



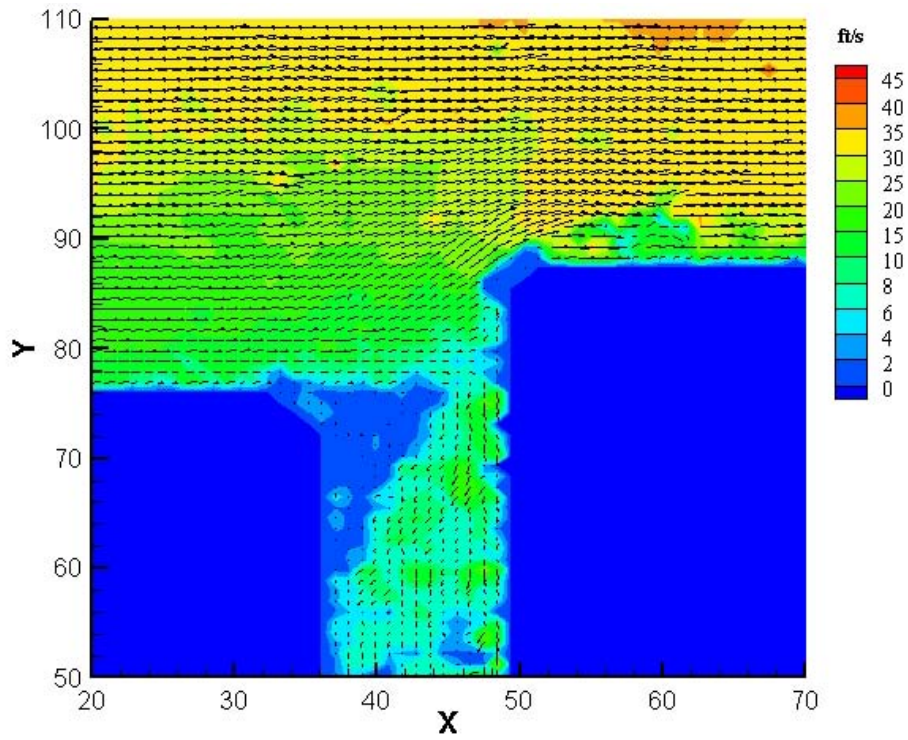
(a)



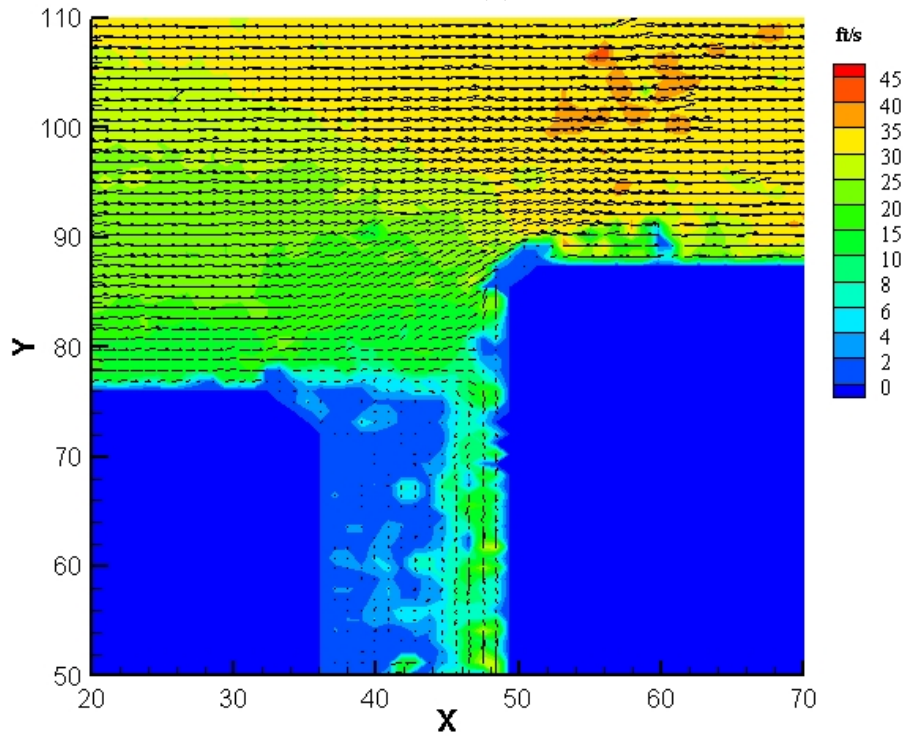
(b)

Figure 40.—Velocity fields for the ½-inch gap and ½-inch chamfered offset at 20-ft/s free stream velocity test conditions: (a) vented and (b) sealed cavity.

Uplift and Crack Flow Resulting from
High Velocity Discharges over Open Offset Joints



(a)



(b)

Figure 41.—Velocity fields for the 1/2-inch gap and 1/2-inch chamfered offset at 30-ft/s free stream velocity test conditions: (a) vented and (b) sealed cavity.

The recirculation zone effect is most evident in figures 42 and 43 that show the horizontal velocity profiles extracted from the PIV results for vented operation (i.e., velocity profiles are along the centerline of the test section). For the $\frac{1}{8}$ -inch gap, a significant difference in velocity profiles exists in comparison with the 20- and 30-ft/s free-stream velocities, the latter producing larger velocities and hence unit discharges. Such results are not observed for the $\frac{1}{2}$ -inch gap, in which case the gap velocity profiles are nearly independent of free-stream velocity. These results have interesting and important implications for unit discharge indicating that for smaller gaps, increased free-stream velocities are expected to produce increased joint/crack unit discharges. However, as the gap increases, there is less sensitivity in unit discharge with free-stream velocity for the range of conditions tested (i.e., 20- and 30-ft/s). In fact, volumetric flow rate measurements of joint/crack discharges indicate that higher free stream velocities actually produce lower joint/crack unit discharges. Again, such results are physically reasonable owing to the observed recirculation zone for the $\frac{1}{2}$ -inch gap configuration and increased changes in momentum required for increased free-stream velocities. There is expected to be a minimum joint/crack size where the internal resistance within the crack becomes the controlling factor.

With regard to uplift pressure specifically, it is less evident how these reported velocity field characteristics directly affect pressure distributions on the upper and lower surfaces of the downstream slab. In comparison of vented and sealed cavity operations, slight increases in velocity are observed just downstream of the offset slab leading edge. However, there is little evidence of changes in the extent of the separation zones even though larger separation zones are expected for larger free-stream velocities. Thus, from a qualitative perspective, it can only be interpreted that the increases in free-stream velocity downstream of the joint/crack are likely to decrease static pressures along the top surface of offset slab. This, combined with stagnation at the leading edge (offset face) resulting in large pressures transmitted to the cavity below the slab, has the potential to increase uplift pressures for sealed cavity operation in comparison with vented conditions.

Uplift and Crack Flow Resulting from
High Velocity Discharges over Open Offset Joints

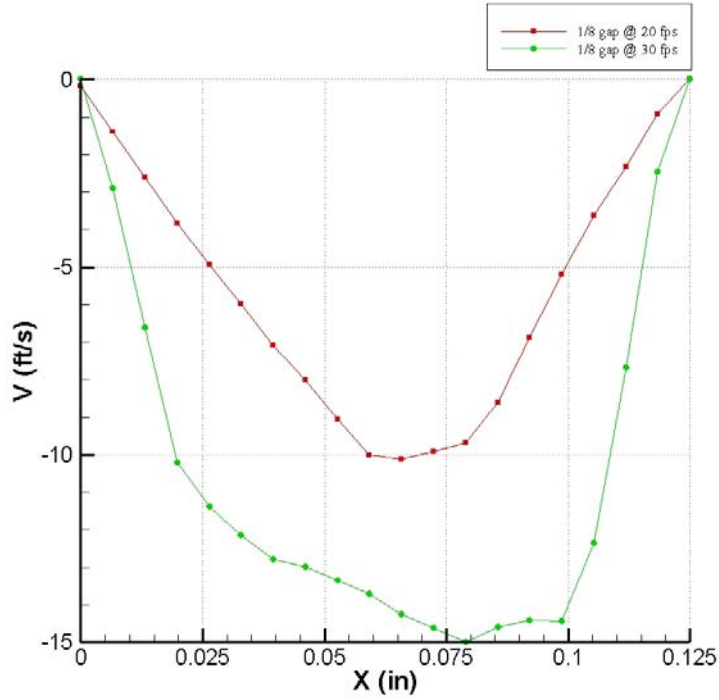


Figure 42.—Joint/crack velocity profiles for the vented 1/8-inch gap configuration with test velocities of 20 and 30 ft/s.

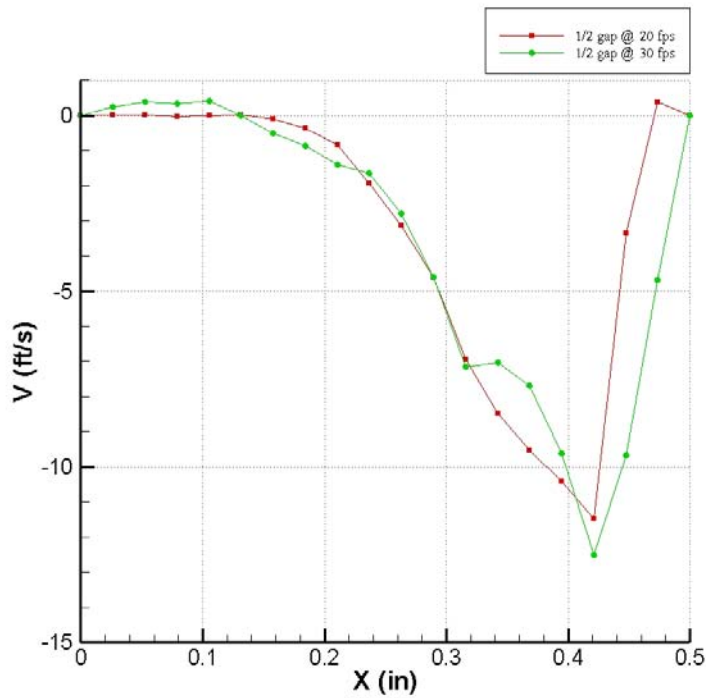


Figure 43.—Joint/crack velocity profiles for the vented 1/2-inch gap configuration with test velocities of 20 and 30 ft/s.

Numerical Modeling

Results of the CFD modeling performed with Flow-3D will be presented in two sections: prototype chute modeling and laboratory test facility modeling.

Prototype Chute CFD Modeling

Several conditions were run for the prototype chute configuration. All these conditions featured a free-surface flow with depths of 2, 6, 12, and 24 inches, a $\frac{1}{8}$ -inch offset into the flow, and a $\frac{1}{8}$ -inch joint/crack gap for flow velocities of 10, 50, and 90 ft/s. Variations in the depth did not provide considerable differences except for the increase in pressure due to the hydrostatic component. Examples of the CFD results (figs. 44 through 49) are presented here for the 12-inch flow depth at all three velocities tested both for a sealed cavity (representing no flow through the joint/crack) and for atmospheric pressure in the cavity (representing maximum flow through the joint/crack that is physically possible). These simulations also show the variation in uplift pressure with distance downstream from the offset joint. The small area of high magnitude uplift forces caused by separation at the offset could have substantial impact on possible failures depending on the geometry that is present; however, the pressure recovers rather quickly and gives a result more in line with the mean differential pressure we measured in the laboratory model.

The gap flow predicted by the Flow3D[®] simulation for $\frac{1}{8}$ -inch offset into the flow and $\frac{1}{8}$ -inch gap, 1-foot depth and 10-, 50-, and 90-ft/s appears in figure 50. The lab model data for the same geometry shows the effect of higher losses in the drain system affecting the unit discharge.

Uplift and Crack Flow Resulting from
High Velocity Discharges over Open Offset Joints

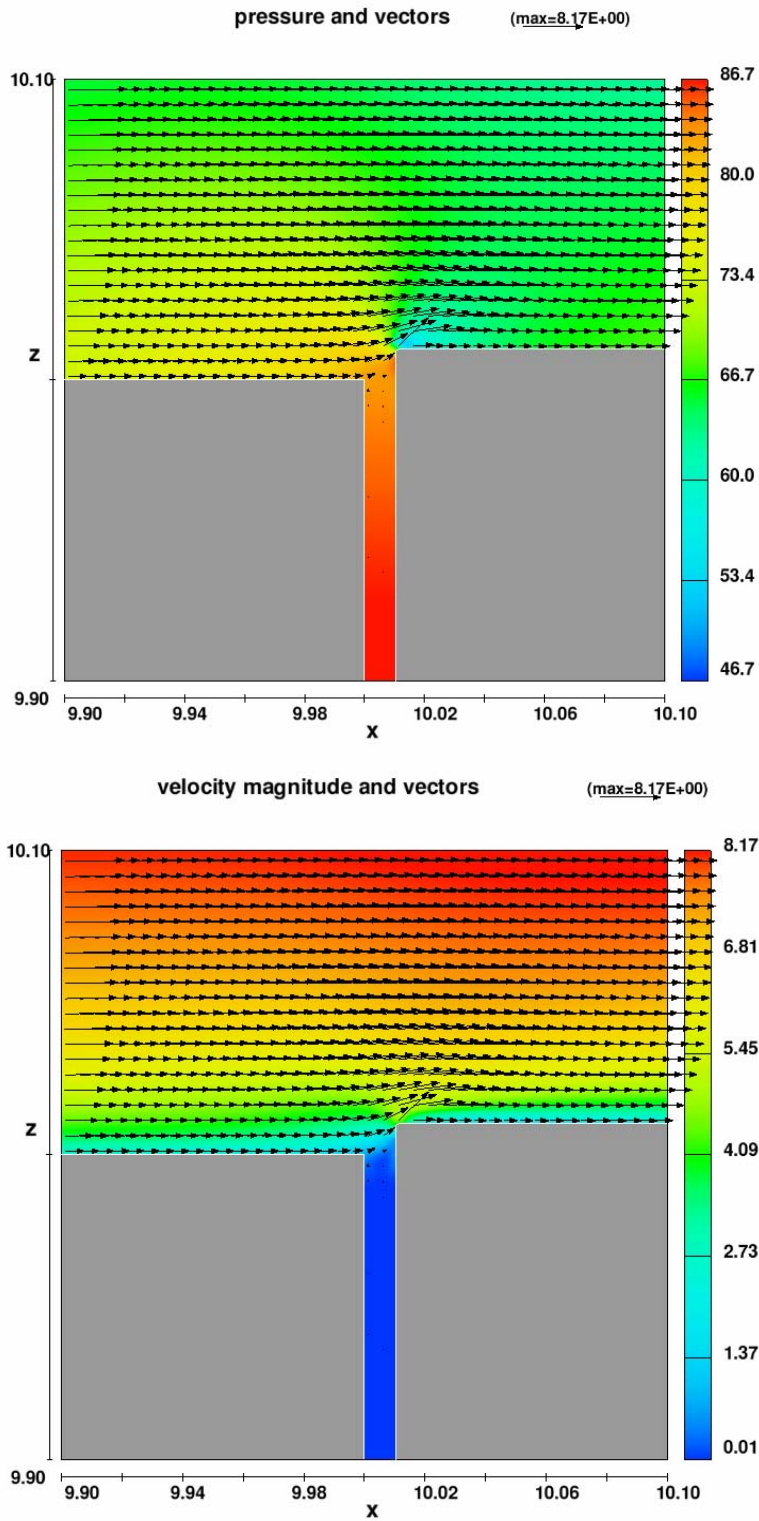


Figure 44.—Prototype chute CFD model results, 12-inch flow depth, 10 ft/s velocity, $\frac{1}{8}$ -inch offset into the flow, $\frac{1}{8}$ -inch joint/crack gap, sealed cavity. Pressures are in lb/ft^2 , and velocity in ft/s.

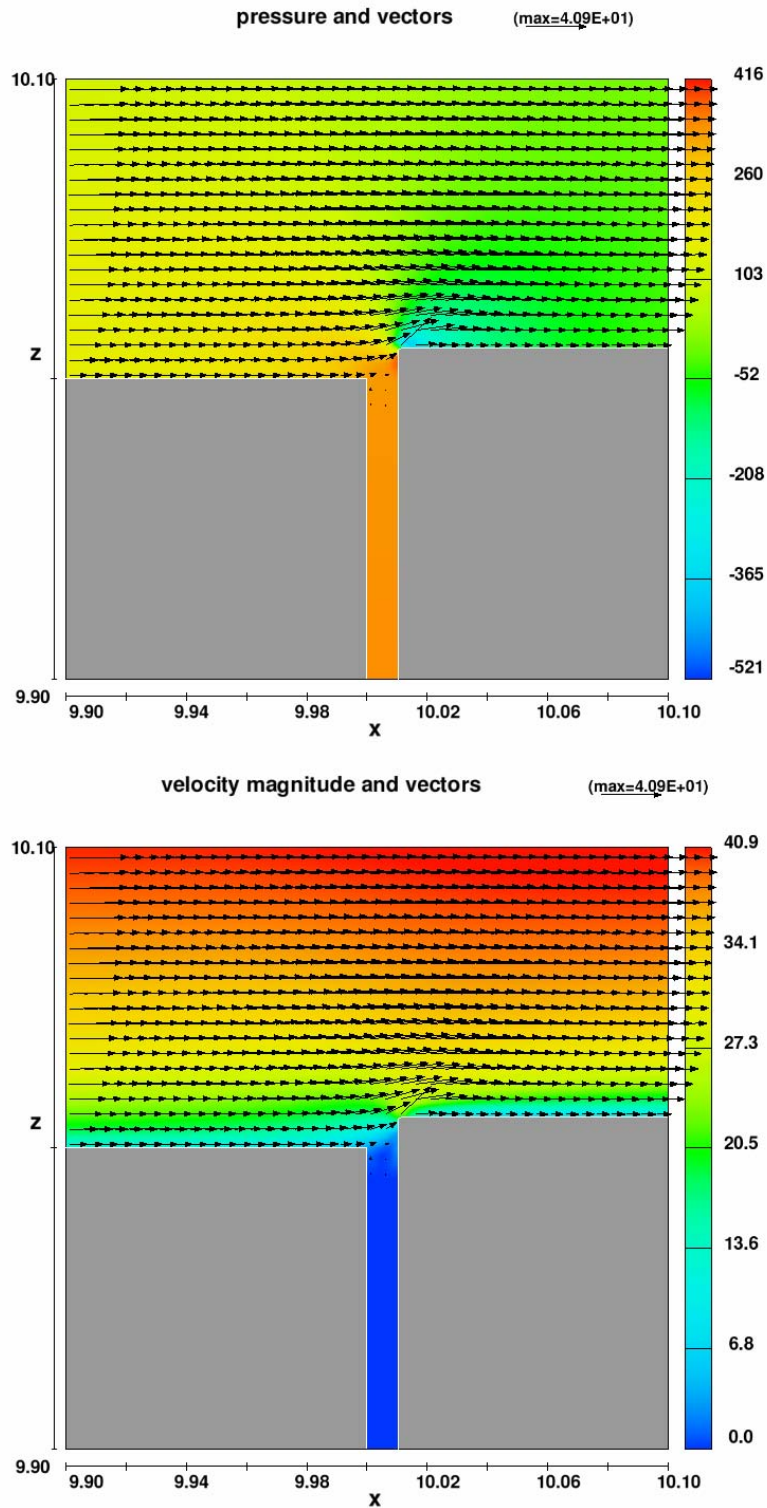


Figure 45.—Prototype chute CFD model results, 12-inch flow depth, 50 ft/s velocity, 1/8-inch offset into the flow, 1/8-in joint/crack gap, sealed cavity. Pressures are in lb/ft², and velocity in ft/s.

Uplift and Crack Flow Resulting from
High Velocity Discharges over Open Offset Joints

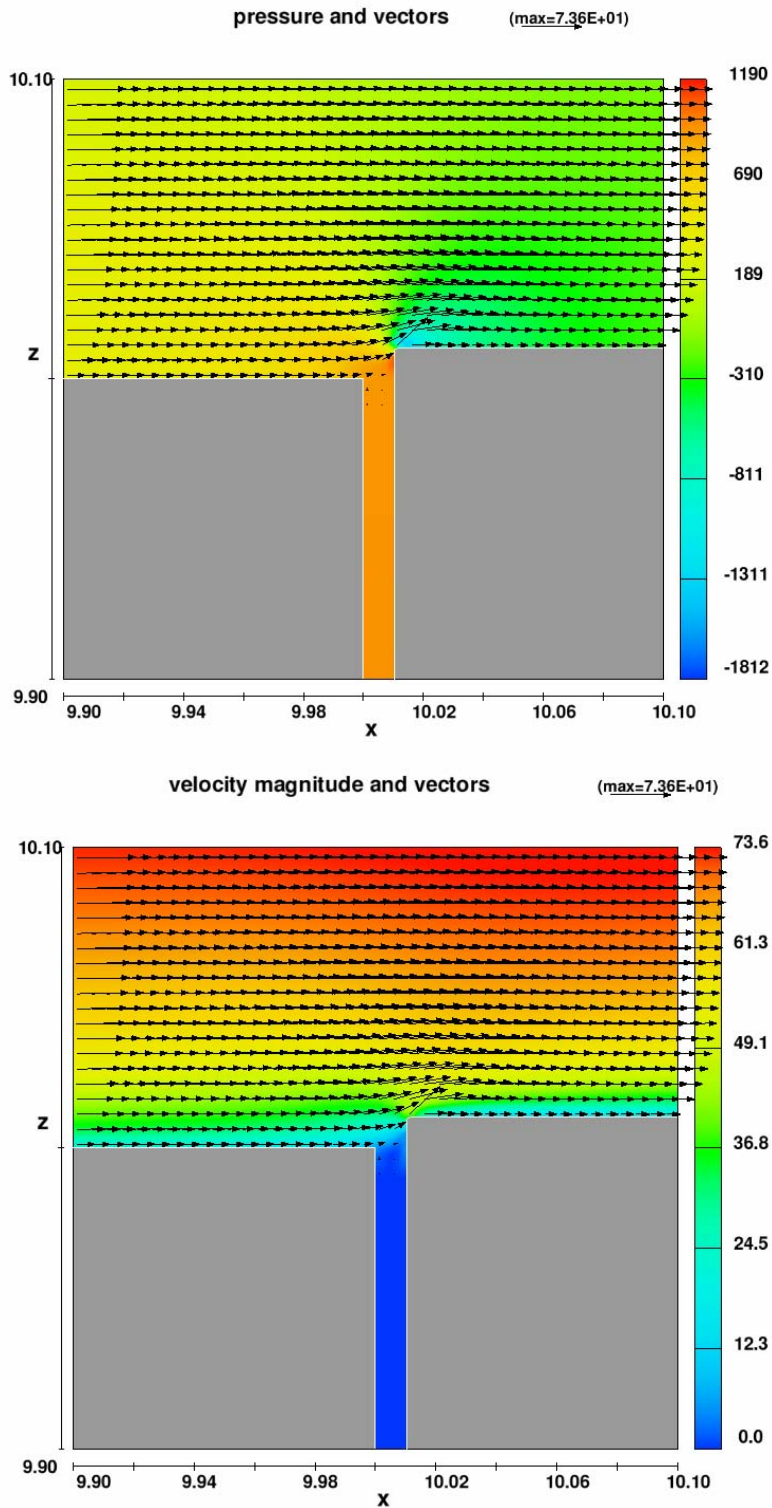


Figure 46.—Prototype chute CFD model results, 12-inch flow depth, 90 ft/s velocity, $\frac{1}{8}$ -inch offset into the flow, $\frac{1}{8}$ -inch joint/crack gap, sealed cavity. Pressures are in lb/ft^2 , and velocity in ft/s . Pressures are in lb/ft^2 , and velocity in ft/s .

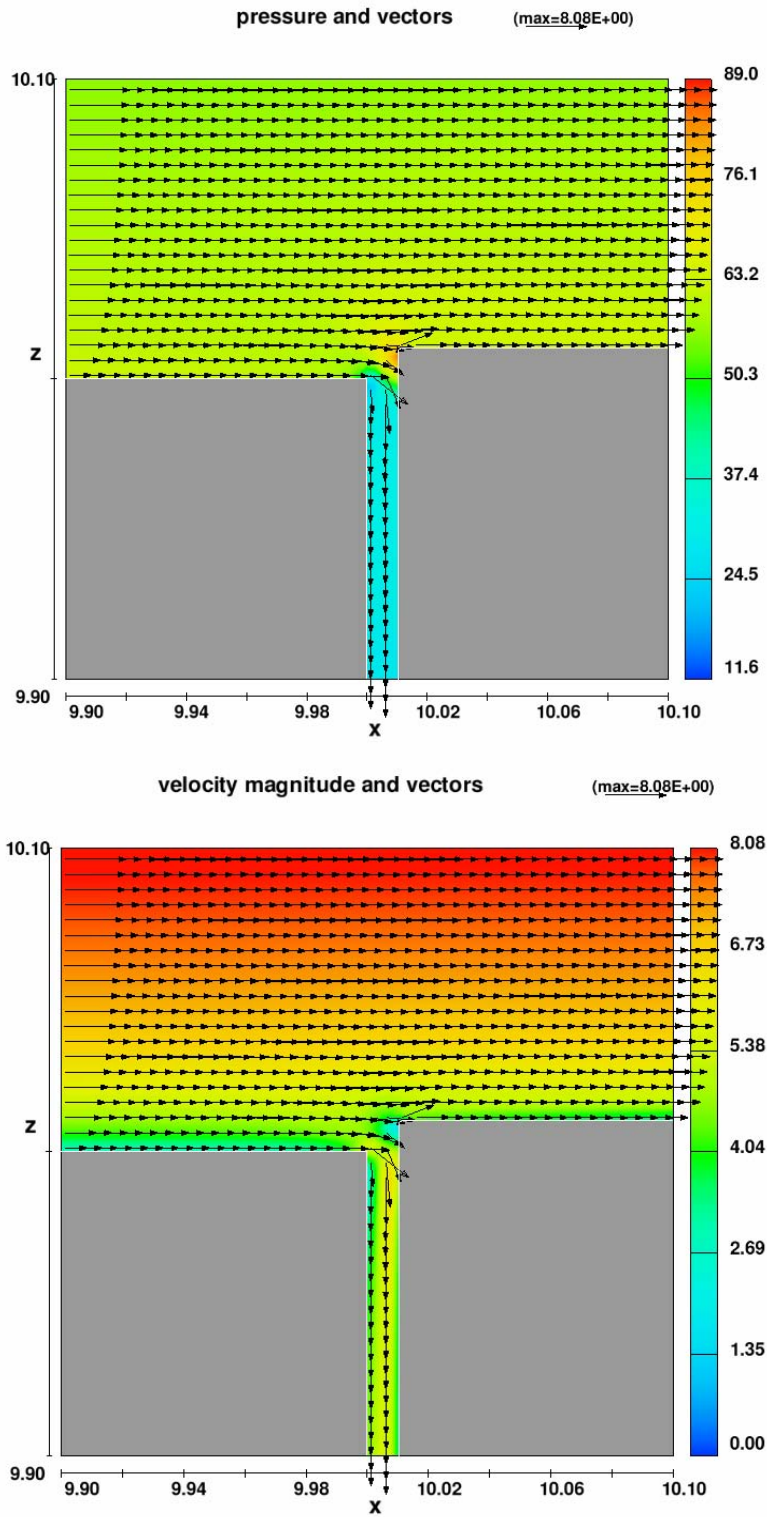


Figure 47.—Prototype chute CFD model results, 12-inch flow depth, 10 ft/s velocity, 1/8-inch off Pressures are in lb/ft², and velocity in ft/s.et into the flow, 1/8-inch joint/crack gap, flow in joint/crack to atmospheric pressure (worst case).

Uplift and Crack Flow Resulting from
High Velocity Discharges over Open Offset Joints

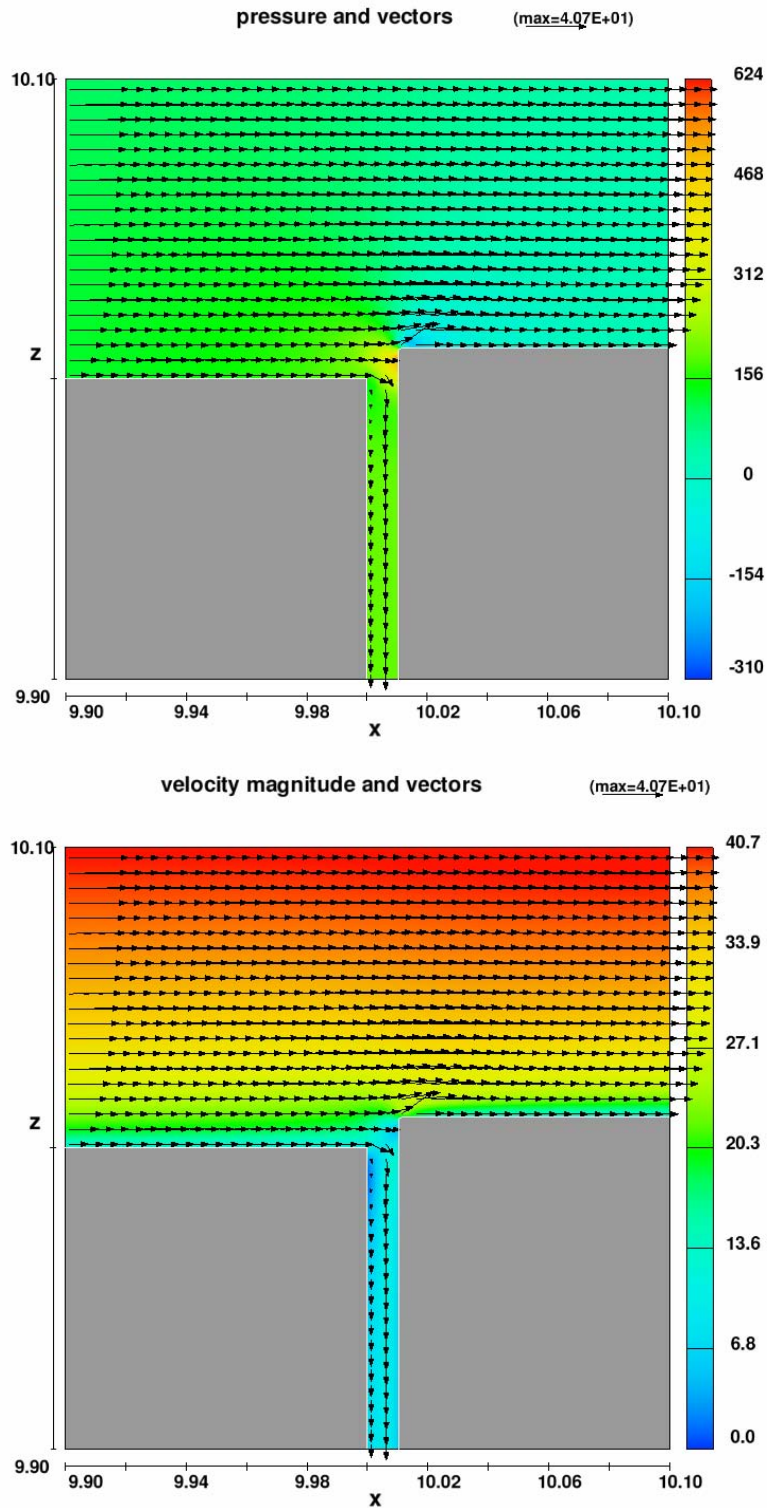


Figure 48.—Prototype chute CFD model results, 12-inch flow depth, 50 ft/s velocity, $\frac{1}{8}$ -inch offset into the flow, $\frac{1}{8}$ -inch joint/crack gap, flow in joint/crack to atmospheric pressure (worst case). Pressures are in lb/ft^2 , and velocity in ft/s .

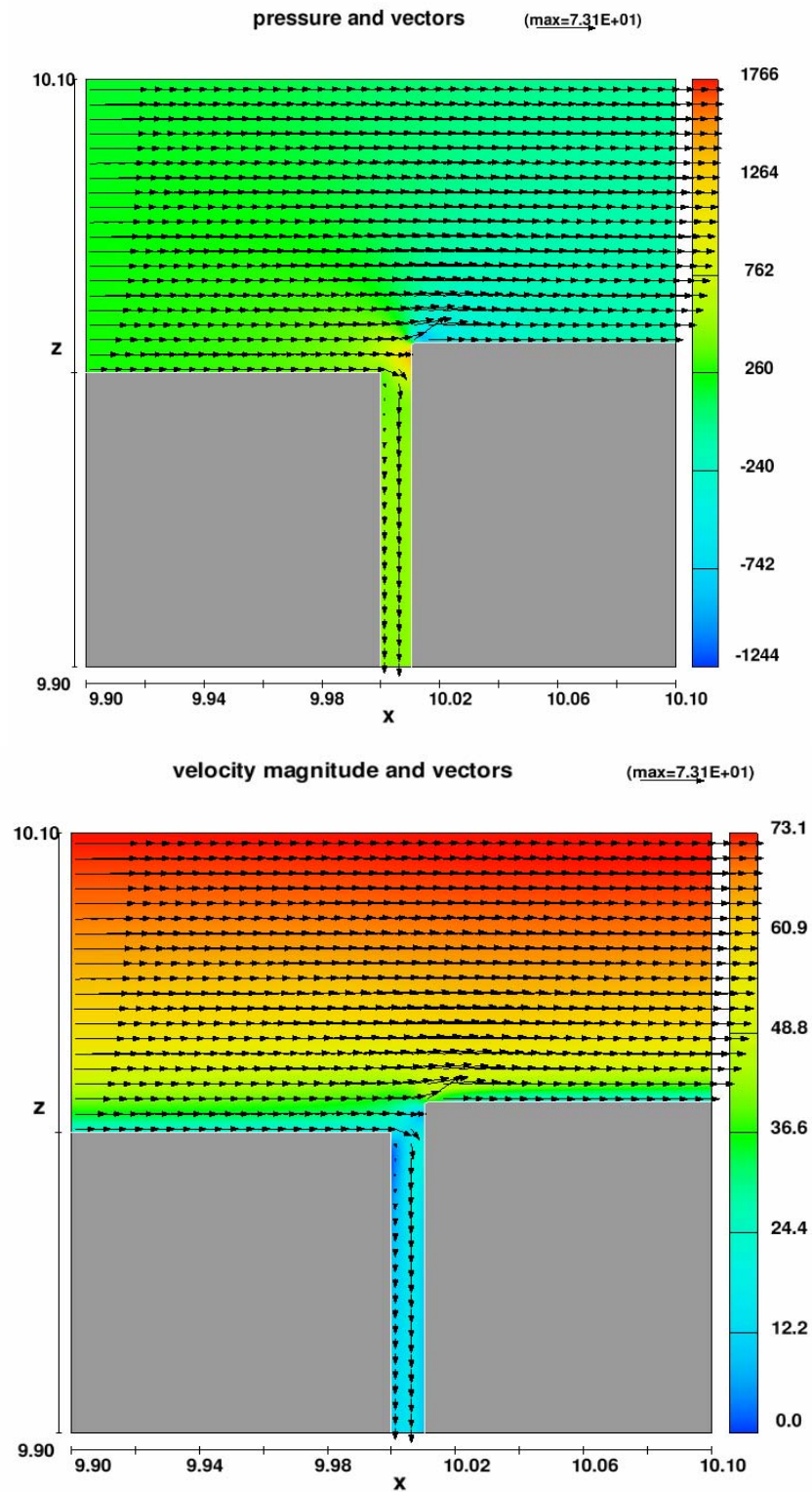


Figure 49.—Prototype chute CFD model results, 12-inch flow depth, 90 ft/s velocity, $\frac{1}{8}$ -inch offset into the flow, $\frac{1}{8}$ -inch joint/crack gap, flow in joint/crack to atmospheric pressure (worst case). Pressures are in lb/ft^2 , and velocity in ft/s.

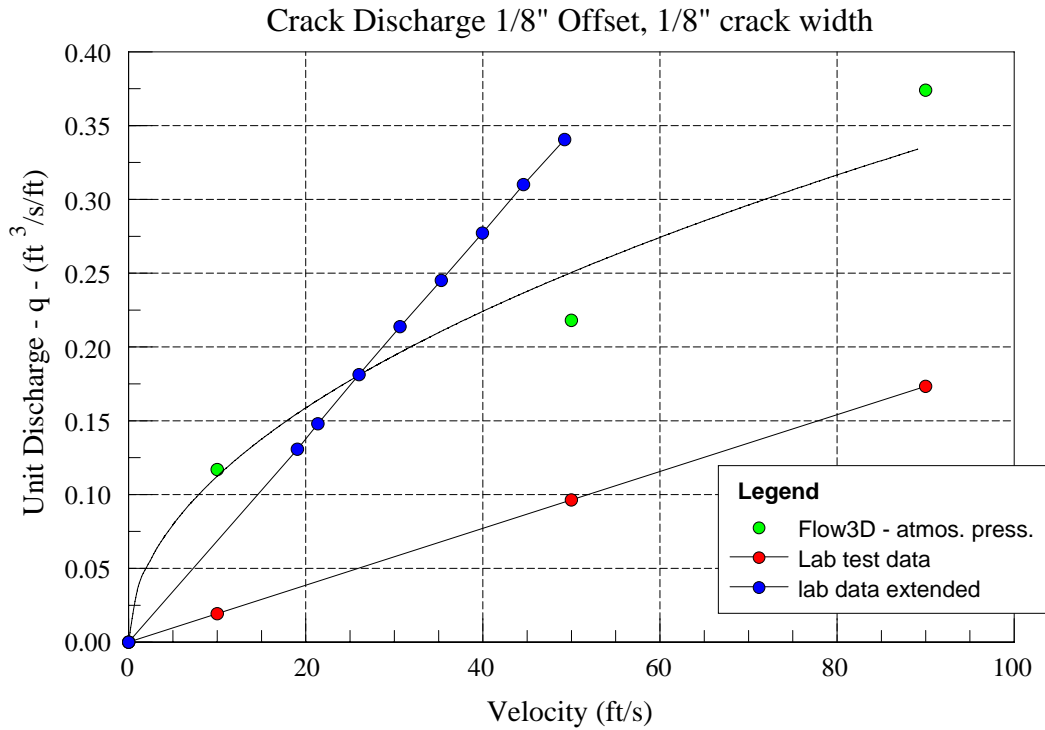


Figure 50.—Unit discharge in joint/crack for 1/8-inch offset and 1/8-inch gap. Free surface simulation with 1-foot depth.

Laboratory Test Facility CFD Modeling

The results presented here are for a mean flow velocity of 50 ft/s, a 1/8-inch offset into the flow, and 1/32-, 1/16-, 1/8-, 1/4-, and 1/2-inch gaps for a sealed cavity. These runs were performed mainly to improve the understanding of how uplift pressures are affected by gap. The results are presented in snapshots in time showing resultant velocity magnitude contours with velocity vectors and pressure contours with velocity vectors overlaid. Figures 51 through 55 show the effect of increasing joint/crack gaps for fixed velocity and offset height.

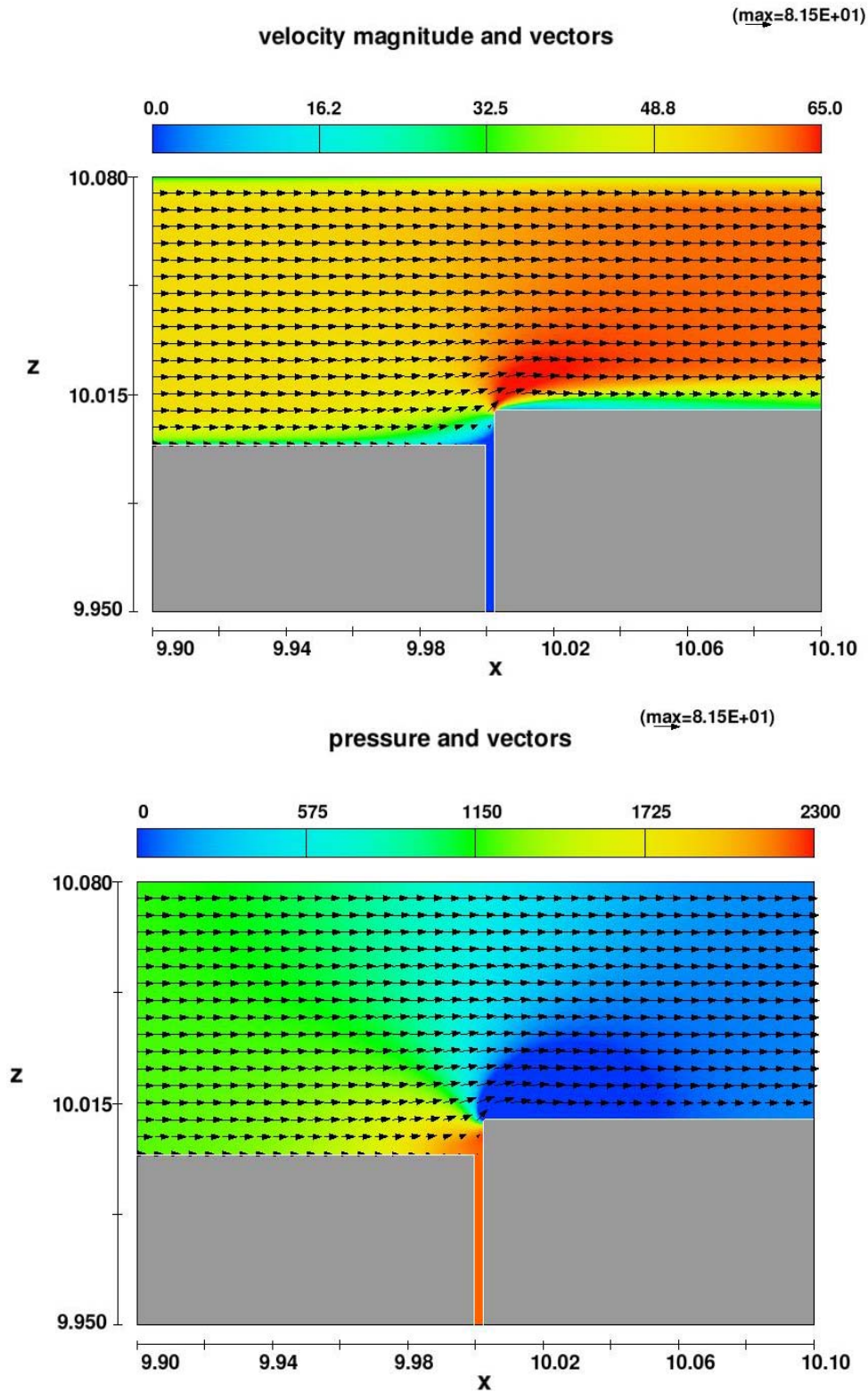


Figure 51.—Laboratory test facility CFD results for a 1/32-inch gap with 1/8-inch offset into the flow for a 50 ft/s velocity. Pressure is in lb/ft² and velocity in ft/s.

Uplift and Crack Flow Resulting from
High Velocity Discharges over Open Offset Joints

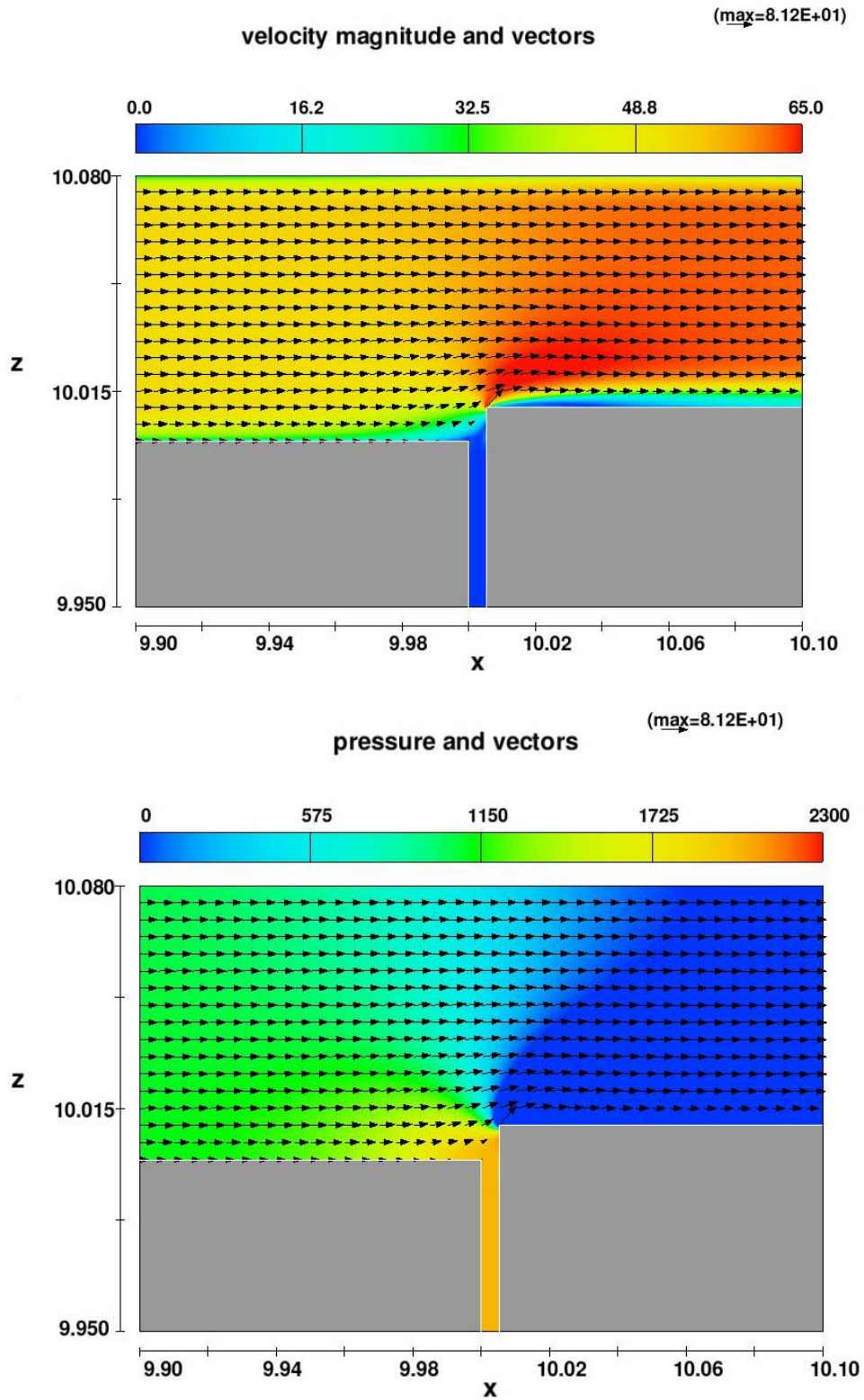


Figure 52.—Flow3D simulation of 1/16-inch gap with 1/8-inch offset into the flow for a 50 ft/s velocity. Pressure is in lb/ft² and velocity in ft/s.

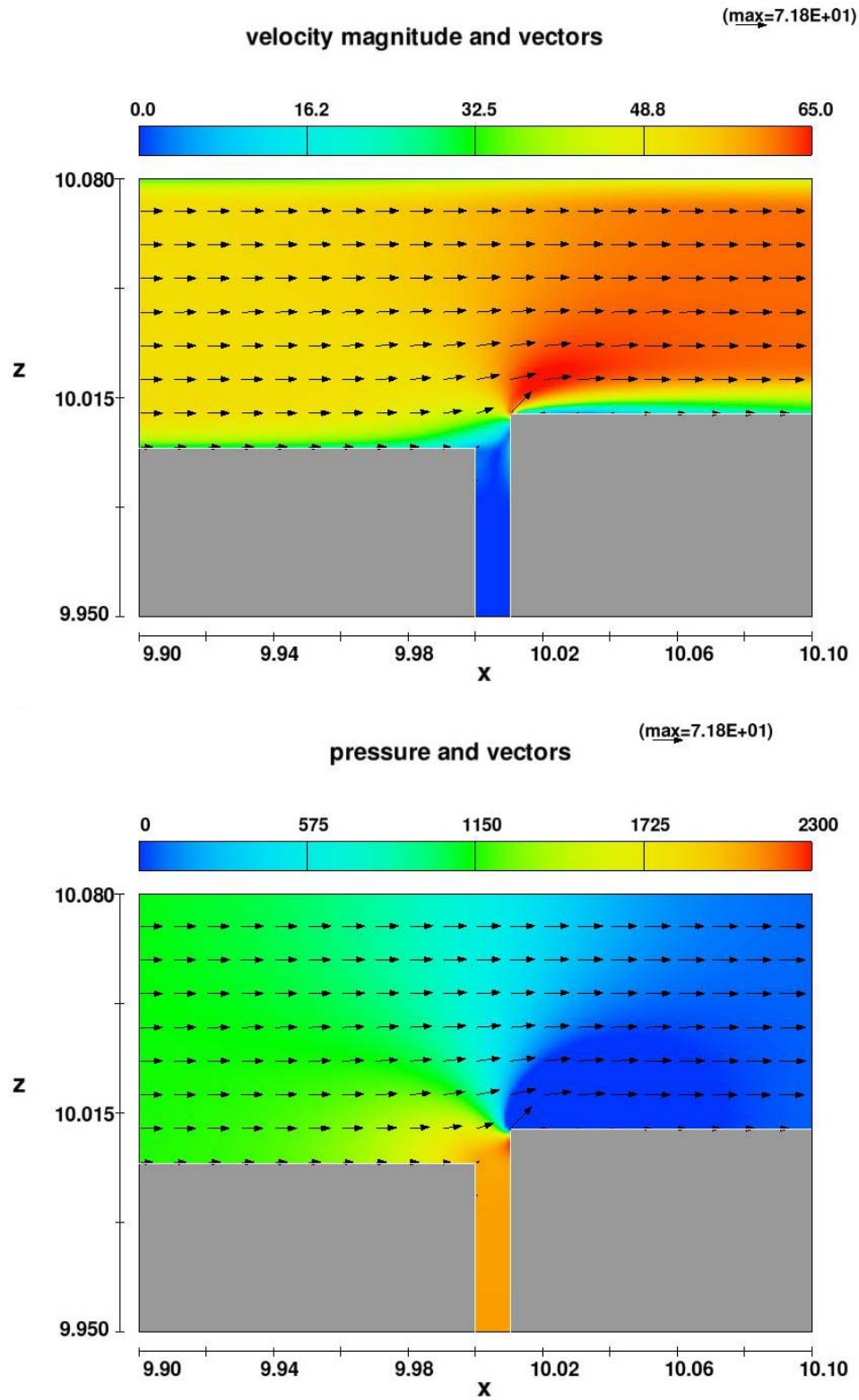


Figure 53.—Flow3D simulation of $\frac{1}{8}$ -inch gap with $\frac{1}{8}$ -inch offset into the flow for a 50 ft/s velocity. Pressure is in lb/ft² and velocity in ft/s.

Uplift and Crack Flow Resulting from
High Velocity Discharges over Open Offset Joints

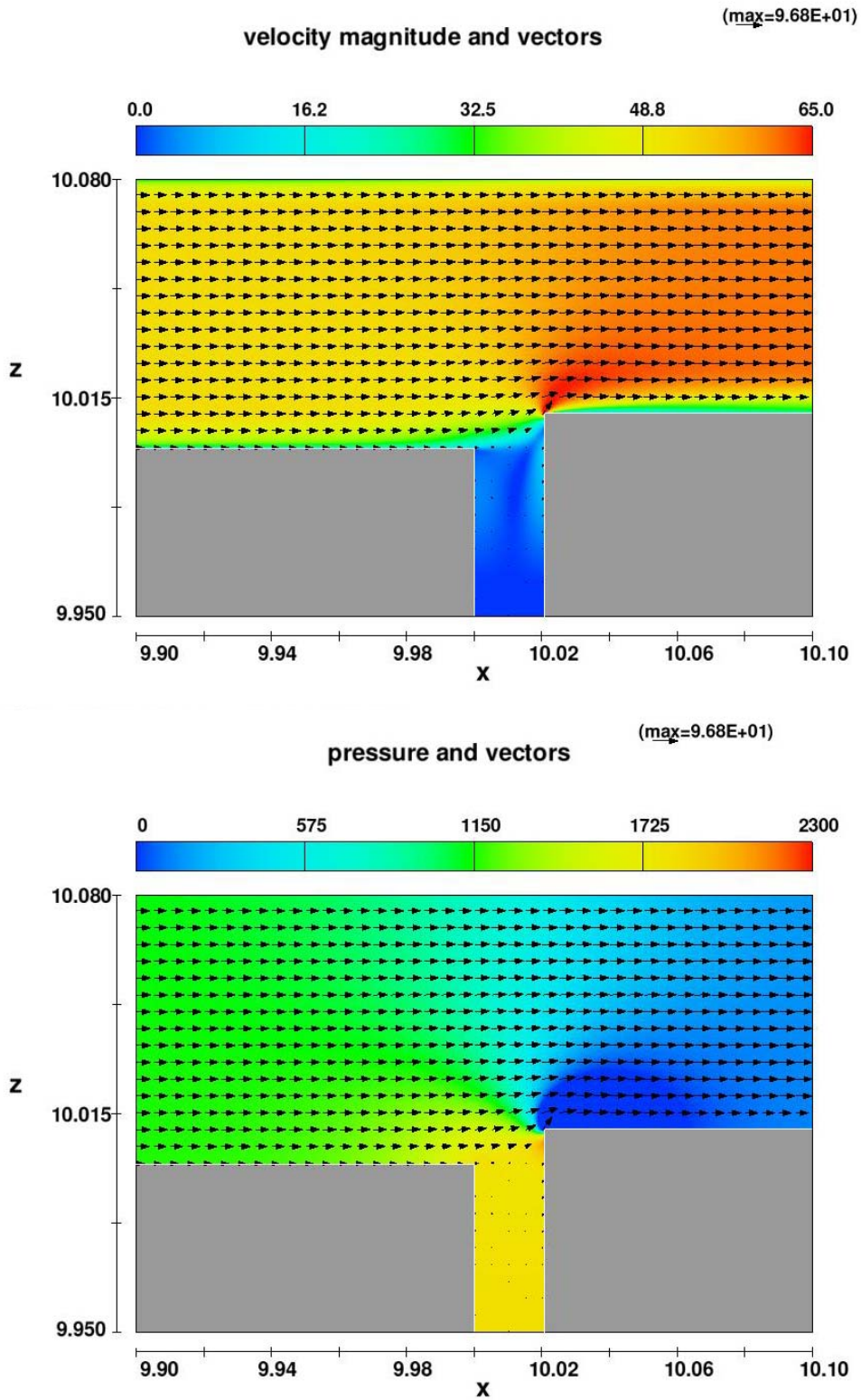


Figure 54.—Flow3D simulation of $\frac{1}{4}$ -inch gap with $\frac{1}{8}$ -inch offset into the flow for a 50 ft/s velocity. Pressure is in lb/ft^2 and velocity in ft/s .

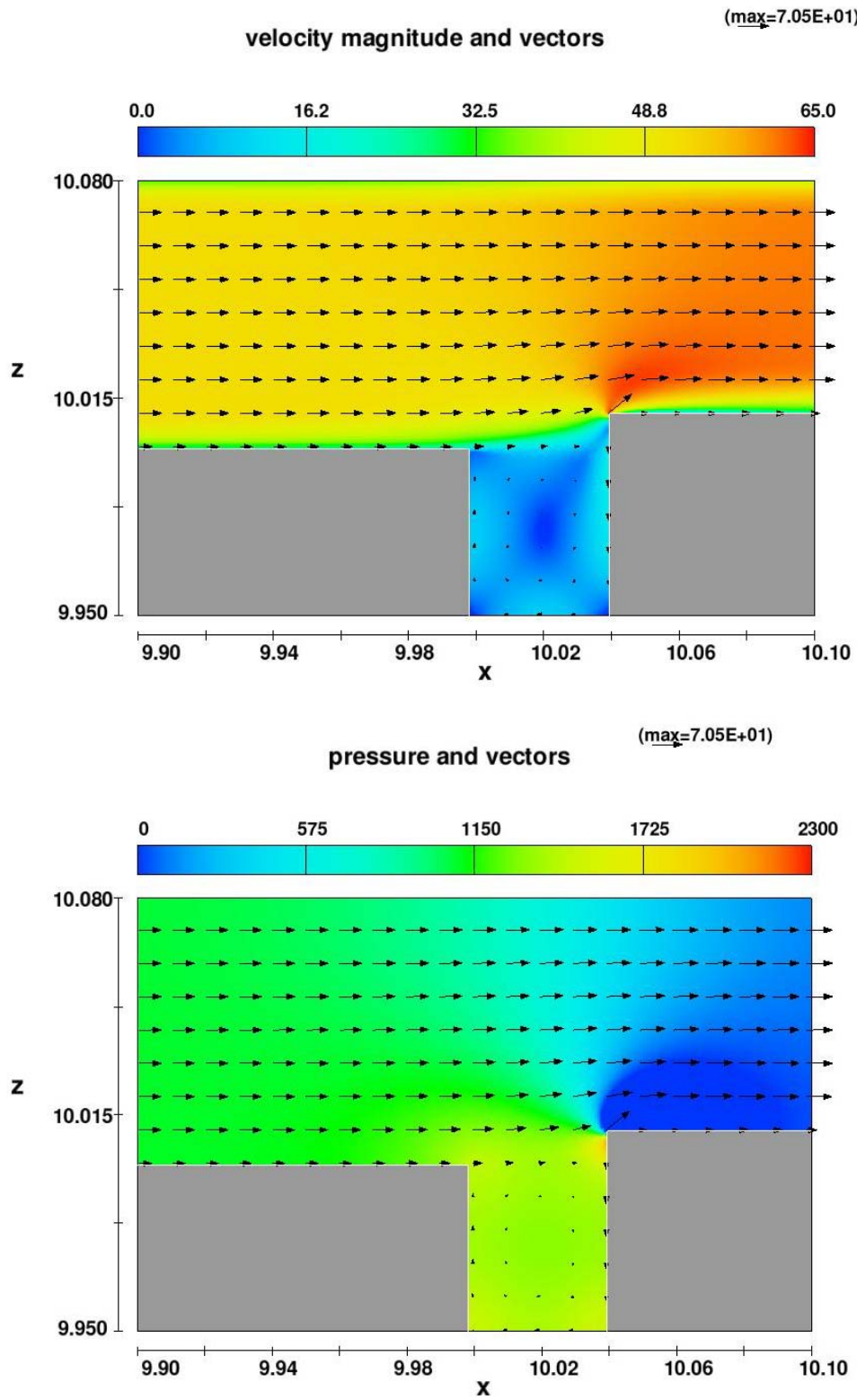


Figure 55.—Flow3D simulation of 1/2-inch gap with 1/8-inch offset into the flow for a 50 ft/s velocity. Pressure is in lb/ft² and velocity in ft/s.

Discussion

The tests performed during this research study should provide increased insight into the behavior of uplift pressures and joint/crack flows for a variety of joint parameters. Increased knowledge of how joints and/or cracks transmit both pressures and flows beneath a slab is of particular value to those tasked with evaluating maintenance or repair/replacement scenarios that may result from a recommendation of a Comprehensive Facility Review (CFR), Issue Evaluation (IE), or a Corrective Action Study (CAS). Better estimates of possible problems resulting from uplift pressures or flows will reduce the uncertainties that engineers are faced with when performing risk-based analyses. The work presented here is not without limitations and definitely does not address every possible scenario that could occur in a field installation.

Prior to this work, many of the recent decisions regarding potential uplift have been largely based on work performed by Johnson (1976) as part of Reclamation's Open and Closed Conduit Systems Committees' (OCCS) research program. Hepler and Johnson (1988) further applied and documented this research in a paper where its application to spillway failures was presented. Others within Reclamation have used these data, rearranged graphing parameters, and analytically extended the range to produce a set of graphs for varying horizontal offsets (Trojanowski, 2004); figure 56 shows this result for 1/8-inch gaps.

The major question regarding the use of these data has always been in the scale-up process. Data were limited to a model velocity of 15 ft/s, and then Froude number-based scaling laws were used to extend the data to the higher velocities reminiscent of typical spillway flows.

The generation of hydraulically produced uplift pressures relies on a break in the continuity of the lining and some feature that transfers the effective pressure of the flowing water below the lining. These breaks in continuity can be at joints or joint/cracks that may have developed. The transmission of pressures and flows through a properly designed and constructed joint would also have to rely on lack of integrity of the waterstop, if so designed. While uplift pressures can also be produced due to transmission of reservoir pressures to the area beneath the lining due to seepage or other problems with the reservoir and/or dam, those issues were not addressed in this work. The pressure distribution on the upper surface of the lining due to the flowing water is typically only the static pressure due to depth of flow. The transmission of pressure to the area beneath the lining depends on the gap width, offset height, orientation to the flow direction, and a variety of other less important geometry and flow related features. When an offset surface intercepts flow, velocity is converted to pressure through a process known as stagnation. Treating water as an incompressible fluid, the stagnation pressure is the conversion of velocity to pressure (i.e., it is the dynamic pressure in the flow

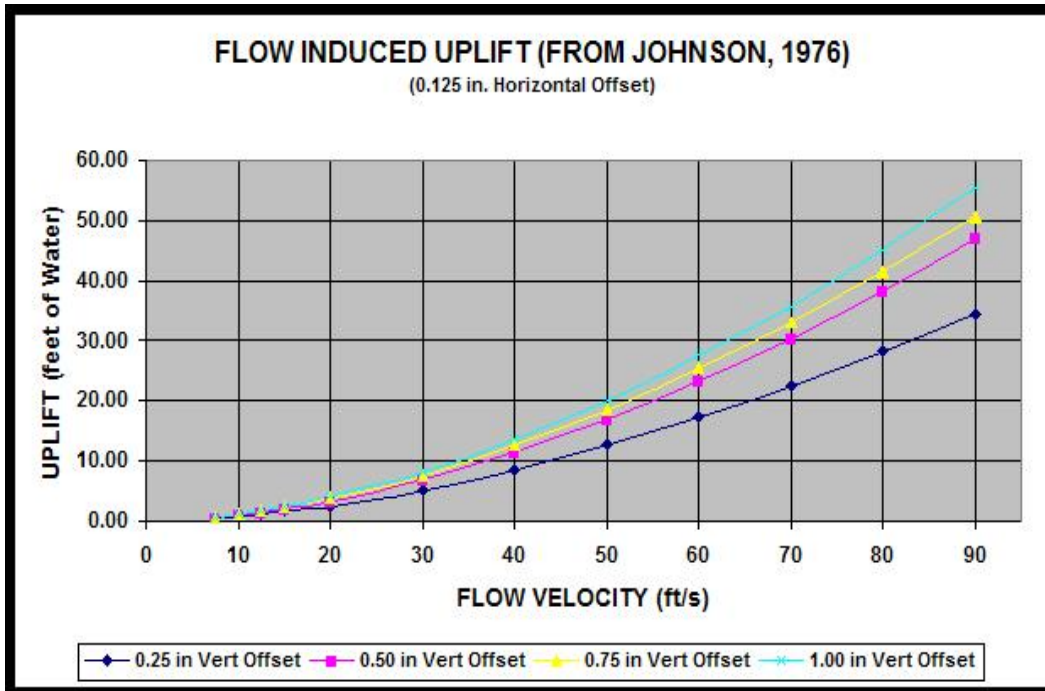


Figure 56.—Graph derived from Johnson's work in 1976 on uplift of steep chute lateral linings.

field), and the stagnation point is the location where the velocity goes to zero. The dynamic pressure is defined as:

$$\frac{1}{2} \rho U^2 = p_o - p \quad (2)$$

where ρ is the density, U is the velocity, p is the static pressure, and p_o is the stagnation pressure. In the treatment of the stagnation pressure for this study, the mean free stream velocity was used to compute the maximum stagnation pressure that is physically possible. The actual pressure that a particular sized offset experiences may be quite reduced due to boundary layer development at the particular location on the lining.

Similar trends for the uplift pressure data were found between the sharp-edged joint and Johnson's (1976) data. Although the actual magnitudes differed, the trend for a decrease in uplift pressure with an increase in the horizontal gap dimension for a given offset height was consistently observed during this testing. It may be postulated that this is due to formation of a driven recirculation zone at the point of the gap entrance that effectively blocks transmission of the full stagnation pressure from reaching the area under the lining. This was demonstrated by the PIV results from the laboratory model.

The lab tests also allowed the comparison of some different joint/gap geometry details, namely, a sharp-edged configuration was tested along with $\frac{1}{8}$ -inch

Uplift and Crack Flow Resulting from High Velocity Discharges over Open Offset Joints

chamfered edges and 1/8-inch radii edges. There were significant differences in the pressures and flow rates that were transmitted to the underside of the lining with these different geometries. As the offset height increased, the difference in geometries became less prominent. The most notable effect of the change in geometry from sharp edges to the chamfer and radii was to effectively widen the gap.

Flow into the joint gap is driven by the stagnation process for high-velocity flow impacting an offset. When there is a sealed cavity beneath the slab, this velocity is converted to pressure and an increase in the uplift pressure is observed. If flow is possible into the cavity, there are a couple of different controlling factors; most notable are losses through the gap, which control the flow (this may be the case for very small gap dimensions), or flow is controlled by losses in the “drain system” downstream from the gap. The laboratory model for all configurations tested had the total gap flows controlled by the drain system. On the contrary, the CFD model results for the prototype chute represented atmospheric pressure at the gap flow boundary, thus creating the maximum possible pressure difference to drive flow into the gap. In such a case, the gap dimensions control the magnitude of flow (see fig. 50, showing a comparison of measured and CFD-predicted unit discharges for the lab model with the same geometry). It should be noted that for the case where the drainage system controls gap flow rates, the uplift pressures are larger than for the case of maximum possible gap discharge. In other words, increased gap discharges are the result of reduced uplift pressures due to adequate drainage for fixed geometries, flow depths, and free-stream velocities.

Finally, it is important to note that changes in offset slab inclination and the effect of turbulent fluctuations were not investigated, but potentially have a significant influence on uplift pressures. Depending on frequency and cavity configuration, fluctuation pressures resulting from turbulent flow may produce cavity resonance (an effect that is more likely when gaseous entrainment occurs). Such physical processes have been observed for high-velocity flows in the vicinity of rock fissures (Bollaert, 2002). However, this condition was not included in this study. Furthermore, it can be expected that given the same joint/crack configuration and free-stream velocity, an offset slab declined in the flow direction would produce localized larger uplift pressures as compared with an inclined offset slab. Such an effect would primarily result from flow separation downstream of the leading edge and delayed reattachment leading to a larger region of reduced static pressure along the upper surface.

Adaptation of the results from this study into a spreadsheet application could be accomplished easily to allow for quick evaluations of a given crack or joint condition. If further detailed information is required for a specific site, Flow-3D has shown to give excellent hydraulic-based results. Perhaps of more concern however, is the condition of features that cannot easily be inspected. The underlying joint details, condition of the waterstops (if equipped), and condition of the drainage system are features that are equally important in the overall

evaluation of the spillway or outlet works system and have a direct bearing on the ultimate performance of the hydraulic structure.

Conclusions and Recommendations

The current state of the practice regarding prediction of uplift pressures generated by offset open joints in spillway and outlet works chutes has been advanced by the use of a relatively simple lab model and corresponding numerical studies. The laboratory model provides data on both resulting uplift pressures and flow into the gap for three transverse joint/crack details. The laboratory model featured prototype scale offsets and gaps along with velocities up to 55 ft/s. The pressures and gap flows were both shown to follow physical theory relating to the dominant processes that are involved. Perhaps the most interesting data to come out of the study is the considerable flow that is possible to induce through the gap into the subsurface drainage system. Most drainage designs are not meant to provide for this amount of inflow so they likely will be undersized and pressurized by the incoming flow. This condition, while it is draining some of the gap flows, still results in elevated uplift pressure conditions that vary with the losses in the system.

Many joint/crack configurations were not tested in these studies due to limitations of the facility. Particularly of interest may be the effect of angle of the joint/crack to the flow, although the perpendicular gap tested in these studies would likely feature the highest uplift pressures generated along with the highest gap flows. Joint/crack lines parallel to the flow will result in reduced uplift and gap flows as the only pressure source driving the increase in pressure or flow is the hydrostatic pressure of the flow on the spillway (i.e., depth), and possibly the abrupt change at the end of a joint/crack. For this case, predictions for inflow may follow measurements and theory developed for surface drainage slots found in highway design.

Future refinements to the data in the form of a predictive spreadsheet will provide an excellent tool for the use of quick determinations of possible failure modes for spillway and outlet works slabs due to uplift or possible structural collapse at the risk assessment level. While this work has begun, additional programming is still necessary to provide a complete product. If a specific arrangement or site needs to be evaluated to a finer degree, Flow-3D has shown to be a computational tool that can provide timely and cost effective results that engineers can use to make accurate and informed decisions.

References

Bollaert, Erik, "Transient water pressures in joints and formation of rock scour due to high-velocity jet impact." *These EPFL*, No. 2548, 2002.

Hepler, Thomas E., and Perry L. Johnson, "Analysis of Spillway Failures by Uplift Pressure," *Proceedings of the 1988 National Conference on Hydraulic Engineering*, edited by Steven R. Abt and Johannes Gessler, ASCE, New York, NY: 857-866, 1988.

Johnson, Perry L, "Research into Uplift on Steep Chute Lateral Linings," *Memorandum to the Open and Closed Conduit Systems Committee*, Bureau of Reclamation, Denver CO, July 15, 1976.

Melo, J.F., A.N. Pinheiro, and C.M. Ramos, "Forces on Plunge Pool Slabs: Influence of Joint Location and Width," *J. Hydr. Engrg.*, Volume 132, Issue 1, January 2006: 49-60.

Trojanowski, J., "Assessing Failure Potential of Spillways on Soil Foundation," *Association of State Dam Safety Officials Annual Conference*, Phoenix AZ, September 26-29, 2004.